Available online at www.sciencedirect.com
SCIENCE DIRECT®
Journal of Computational Physics 191 (2003) 147–176
JOURNAL OF COMPUTATIONAL PHYSICS
www.elsevier.com/locate/jcp

Numerical solution to the time-dependent Maxwell equations in axisymmetric singular domains: the singular complement method

F. Assous [a], P. Ciarlet Jr. [b], S. Labrunie [c], J. Segré [a,*]

[a] *Département de Physique Théorique et Appliquée, CEA/DAM Ile-de-France, BP12-F91680 Bruyères-le-Châtel, France*
[b] *ENSTA & CNRS UMR 2706, 32, boulevard Victor, 75739 Paris Cedex 15, France*
[c] *Univ. Henri Poincaré Nancy I, IECN, 54506 Vandœuvre-lès-Nancy Cedex, France*

Received 14 October 2002; received in revised form 15 May 2003; accepted 16 May 2003

Abstract

In this paper, we present a method to solve numerically the axisymmetric time-dependent Maxwell equations in a singular domain. In [Math. Methods Appl. Sci. 25 (2002) 49; Math. Methods Appl. Sci. 26 (2003) 861], the mathematical tools and an in-depth study of the problems posed in the meridian half-plane were exposed. The numerical method and experiments based on this theory are now described here. It is also the generalization to axisymmetric problems of the *Singular Complement Method* that we developed to solve Maxwell equations in 2D singular domains (see [C. R. Acad. Sci. Paris, t. 330 (2000) 391]). It is based on a splitting of the space of solutions in a regular subspace, and a singular one, derived from the singular solutions of the Laplace problem. Numerical examples are finally given, to illustrate our purpose. In particular, they show how the *Singular Complement Method* captures the singular part of the solution.

AMS: 65P25; 77C10

Keywords: Maxwell equations; Axisymmetry; Singularities; Conforming finite element method

1. Introduction

In the recent years, an ever-growing number of engineering problems requiring to model and to simulate numerically devices working with or within electromagnetic fields have come out. The mathematical models describing the physics of these devices are based on Maxwell equations, in the steady-state or time-dependent form, often coupled with other equations.

* Corresponding author. Tel.: +33-1-6908-4800; fax: +33-1-6908-9696.
E-mail addresses: franck.assous@cea.fr (F. Assous), ciarlet@ensta.fr (P. CiarletJr.), labrunie@iecn.u-nancy.fr (S. Labrunie), jacques.segre@cea.fr, segre@soleil.serma.cea.fr (J. Segré).

0021-9991/$ - see front matter
doi:10.1016/S0021-9991(03)00309-7

Moreover, many structures that are to be modeled have a complex three-dimensional geometry and often present a surface with edges and/or corners. These geometrical singularities can generate very strong fields that have to be taken into account. They can be desired, as an active part of the device (e.g., to extract electrons from a cathode), or the consequence of a priori constraints on the design. In that case, the induced negative effects (e.g., destructive effects) have to be controlled.

However, three-dimensional computations are very expensive. In a number of cases, one reduces the problem to two-dimensional equations by assuming that the geometry and the data and initial conditions are independent of one of the coordinates.

As a first step, we considered in a previous paper [4] problems independent of the transverse variable z, which can be reduced to two-dimensional Cartesian ones. We proposed a method, called the *Singular Complement Method* (latter referred to as the *SCM*), which allows to solve Maxwell equations in a *non-smooth and non-convex* domain, that is a *singular* domain.

In this paper, we consider the case of an axisymmetric situation. Indeed, while the geometry of real devices is not very often Cartesian, it is much more common to have an axial symmetry, at least approximately or locally. Moreover, it is a common practice to approximate problems by their axisymmetric counterpart. In other words, the axisymmetric situation can be viewed as an intermediate between a full three-dimensional problem and a two-dimensional one.

Recall briefly the principle of the *SCM*: the space of solutions V is split *with respect to regularity* in a regular subspace V_{R} and a singular one V_{S}, namely $V = V_{\mathrm{R}} \oplus V_{\mathrm{S}}$. When the domain is *convex or smooth*, that is *regular*, there is no singularity in the solutions of the Maxwell equations, so that $V_{\mathrm{S}} = \{0\}$ and $V_{\mathrm{R}} = V$.

Thus, in this case, one can take advantage of this regularity to discretize the electromagnetic fields by the P_1 Lagrange FEM (cf. [5]), instead of the 'usual' edge FEM [20,21]. As a matter of fact, the former discretization includes two key ingredients, which the latter lacks [1]:

- For the time-dependent Maxwell equations, the mass matrix can be lumped, with no loss in precision, thus leading to very inexpensive numerical schemes.
- The numerical electromagnetic field is continuous, so the method can be used in conjunction with a particle-pushing scheme, to solve the coupled Vlasov–Maxwell system of equations.

Alternative approaches, such as Finite Volumes [17], also lack the crucial continuity property of the numerical approximation, and moreover require some charge correction at every time-step.

In general, when the domain is singular, V_{R} is strictly included in V (and $\overline{V_{\mathrm{R}}} \neq V$), and one *cannot capture numerically* the singular part of the solution with the help of the Lagrange FEM only, since the solution cannot arise as a limit of regular fields. In particular, mesh refinement techniques *do not work*.

The principle of the *SCM* being to enlarge the space of test-functions, it is therefore required that one adds a singular complement to be able to compute an approximation of the solution. One discretizes the regular part with the P_1 Lagrange FEM, which means a P_1 approximation component by component, taking into account the boundary condition. To approximate the singular part, the idea we develop further is to relate the singular electromagnetic fields to singular solutions to the Laplace operator. In the axisymmetric situation, all the mathematical tools and characterizations of the singular subspaces of solutions have been carried out and exposed in previous papers [2,3]. For time-dependent problems, another advantage of the *SCM* is that no mesh refinement is needed, so one can use explicit methods without deteriorating the time-step.

Note that we assume that the medium is homogeneous. The extension to heterogeneous media can be dealt with in a similar manner. For that, one can choose the FEM framework developed in [6], in order to handle jumps across interfaces between different media. And, as far as the *SCM* is concerned, one has to compute the singular solutions of elliptic operators with piecewise constant coefficients (see [8]).

[1] Mass lumping techniques are however available for specially designed edge FEM [13].

This paper is organized as follows. Section 2 recalls the time-dependent Maxwell equations in an axisymmetric domain. A decomposition in regular and singular parts is presented in Section 3, where the difference between the electric and the magnetic case is pointed out. A characterization of the fields is given leading to constructive methods of solution. The numerical method is developed in Section 4: the "singular lifting" approach for solving the singular electromagnetic fields, coupled to a time-dependent variational formulation. Section 5 is concerned to the extension of the method to the Silver–Müller boundary condition. In Section 6, we present some numerical results of both electric and magnetic cases, to illustrate the efficiency of the *SCM* in an axisymmetric geometry. In particular, a comparison with a Finite Volume approach [17] is performed.

2. Maxwell equations in an axisymmetric domain

2.1. The Maxwell equations

Let Ω be a bounded and simply connected Lipschitz domain, Γ its boundary, and $\mathbf{n}$ the unit outward normal to Γ. If we let c and ε_0 be, respectively, the speed of light and the dielectric permittivity, the time-dependent Maxwell equations in vacuum read

$$\frac{\partial \mathscr{E}}{\partial t} - c^2 \operatorname{curl} \mathscr{B} = -\frac{1}{\varepsilon_0} \mathscr{J}, \tag{1}$$

$$\frac{\partial \mathscr{B}}{\partial t} + \operatorname{curl} \mathscr{E} = 0, \tag{2}$$

$$\operatorname{div} \mathscr{E} = \frac{\mathscr{R}}{\varepsilon_0}, \tag{3}$$

$$\operatorname{div} \mathscr{B} = 0, \tag{4}$$

where $\mathscr{E}$ is the electric field, $\mathscr{B}$ is the magnetic flux density, and $\mathscr{R}$ and $\mathscr{J}$ are the charge and current densities. These quantities depend on the space variable $\mathbf{x}$ and on the time variable t.

These equations are supplemented with appropriate boundary conditions. In order to simplify the presentation, let us assume first that the boundary is a perfect conductor. In Section 5, the extension to the Silver–Müller boundary condition will be handled: it can model either an absorbing medium outside the domain or an incident wave. For the moment, let us consider the boundary conditions

$$\mathscr{E} \times \mathbf{n} = 0 \quad \text{on } \Gamma, \tag{5}$$

$$\mathscr{B} \cdot \mathbf{n} = 0 \quad \text{on } \Gamma. \tag{6}$$

The charge conservation equation is a consequence of Maxwell equations and reads

$$\frac{\partial \mathscr{R}}{\partial t} + \operatorname{div} \mathscr{J} = 0. \tag{7}$$

Last, initial conditions are provided (for instance at time $t = 0$)

$$\mathscr{E}(0) = \mathscr{E}_0, \quad \mathscr{B}(0) = \mathscr{B}_0, \tag{8}$$

where the couple $(\mathscr{E}_0, \mathscr{B}_0)$ depends only on the variable $\mathbf{x}$ and satisfies the divergence and boundary conditions at the initial time

$$\operatorname{div} \mathscr{E}_0 = \frac{\mathscr{R}(0)}{\varepsilon_0}, \quad \operatorname{div} \mathscr{B}_0 = 0,$$

$$\mathscr{E}_0 \times \mathbf{n} = 0 \quad \text{on } \Gamma, \qquad \mathscr{B}_0 \cdot \mathbf{n} = 0 \quad \text{on } \Gamma.$$

2.2. Reduction to two-dimensional problems

Now we make the supplementary assumption that Ω is an axisymmetric domain limited by the surface of *revolution* Γ. We denote by ω and γ_b their intersections with a meridian half-plane (see Fig. 1). One has $\gamma \overset{\text{def}}{=} \partial\omega = \gamma_a \cup \gamma_b$, where either $\gamma_a = \emptyset$ when γ_b is a closed contour (i.e., Ω does not contain the axis), or γ_a is the segment of the axis lying between the extremities of γ_b. $\boldsymbol{\nu}$ is its unit outward normal and $\boldsymbol{\tau}$ the unit tangential vector such that $(\boldsymbol{\tau}, \boldsymbol{\nu})$ is direct.

Moreover, it is assumed that γ_b is a polygonal line with edges $(\gamma_k)_{1 \leqslant k \leqslant F}$. The off-axis corners of γ_b generate circular edges in Γ, whereas the extremities are conical vertices of Γ.

The natural coordinates for this domain are the cylindrical coordinates (r, θ, z), with the basis vectors $(\mathbf{e}_r, \mathbf{e}_\theta, \mathbf{e}_z)$. A meridian half-plane is defined by the equation $\theta = \text{const.}$, and (r, z) are Cartesian coordinates in this half-plane.

For any vector field $\mathbf{u}$, we denote by $\mathbf{u}_m$ and $\mathbf{u}_\theta$ the meridian and azimuthal components of $\mathbf{u}$, with $\mathbf{u}_m \overset{\text{def}}{=} u_r \mathbf{e}_r + u_z \mathbf{e}_z$ and $\mathbf{u}_\theta \overset{\text{def}}{=} u_\theta \mathbf{e}_\theta$. The fact that there is a *symmetry of revolution* means that the scalar (resp., vector) fields are entirely characterized by their "trace" in ω, i.e., the datum of their value in a meridian half-plane (resp., by the trace of their cylindrical components). Obviously, this is equivalent to the vanishing of all derivatives with respect to θ of these fields or components. In the following, it is thus assumed that $\partial_\theta \cdot = 0$.

The formulae for the gradient, divergence, and curl operators in cylindrical coordinates are given in Appendix A. In the axisymmetric case, we have the following expressions (by using $\partial_\theta \cdot = 0$):

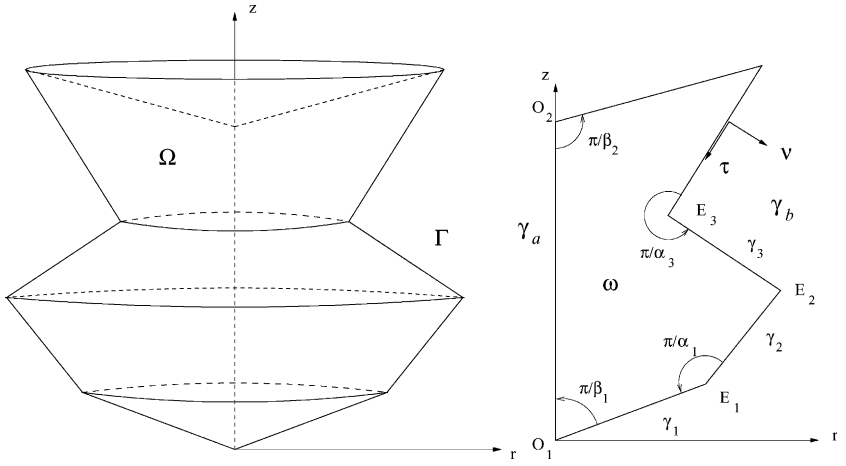

Fig. 1. The domains Ω and ω.

$$\operatorname{grad} f = \frac{\partial f}{\partial r}\mathbf{e}_r + \frac{\partial f}{\partial z}\mathbf{e}_z, \quad \operatorname{div} \mathbf{u} = \frac{1}{r}\frac{\partial}{\partial r}(ru_r) + \frac{\partial u_z}{\partial z}, \tag{9}$$

$$\Delta f = \frac{\partial^2 f}{\partial r^2} + \frac{1}{r}\frac{\partial f}{\partial r} + \frac{\partial^2 f}{\partial z^2}. \tag{10}$$

The curl operator is given by the formula

$$\operatorname{curl} \mathbf{u} = \left(-\frac{\partial u_\theta}{\partial z}\right)\mathbf{e}_r + \left(\frac{\partial u_r}{\partial z} - \frac{\partial u_z}{\partial r}\right)\mathbf{e}_\theta + \frac{1}{r}\left(\frac{\partial}{\partial r}(ru_\theta)\right)\mathbf{e}_z. \tag{11}$$

Now, if $\mathbf{u}_m = (u_r, u_z)$ is a meridian vector field, $\operatorname{curl} \mathbf{u}_m$ is azimuthal. It is thus convenient to introduce the roman type notation

$$\operatorname{curl} \mathbf{u}_m = \left(\frac{\partial u_r}{\partial z} - \frac{\partial u_z}{\partial r}\right).$$

In the same way, if $\mathbf{u}_\theta$ is azimuthal, $\operatorname{curl} \mathbf{u}_\theta$ is meridian and we set, with the bold type notation,

$$\operatorname{curl} u_\theta = -\frac{\partial u_\theta}{\partial z}\mathbf{e}_r + \frac{1}{r}\frac{\partial}{\partial r}(ru_\theta)\mathbf{e}_z.$$

For this reason, it is possible to decouple the Maxwell system (1)–(4) into a couple of problems, involving different components of the fields $\mathscr{E}$ and $\mathscr{B}$. Let us denote by $\mathbf{E}_m = (E_r, E_z)$ (resp., $\mathbf{J}_m = (J_r, J_z)$) the meridian components of $\mathscr{E}$ (resp., $\mathscr{J}$) and by B_θ the azimuthal component of $\mathscr{B}$. Given the expression of differential operators in cylindrical coordinates, the first system of unknowns $(\mathbf{E}_m, B_\theta)$ reads as follows in $\omega\times]0, T[$:

$$\begin{cases} \frac{\partial \mathbf{E}_m}{\partial t} - c^2 \operatorname{curl} B_\theta = -\frac{1}{\varepsilon_0}\mathbf{J}_m, \\ \frac{\partial B_\theta}{\partial t} + \operatorname{curl} \mathbf{E}_m = 0, \\ \operatorname{div} \mathbf{E}_m = \frac{\mathscr{R}}{\varepsilon_0}, \end{cases} \tag{12}$$

with the perfect conductor boundary condition

$$\mathbf{E}_m \cdot \boldsymbol{\tau} = 0 \quad \text{on } \gamma_b. \tag{13}$$

On the axis γ_a, symmetry considerations yield

$$\mathbf{E}_m \cdot \boldsymbol{\nu} = E_r = 0, \quad B_\theta = 0 \qquad \text{on } \gamma_a. \tag{14}$$

We also have the initial conditions

$$\mathbf{E}_m(0) = \mathbf{E}_{m0}, \quad B_\theta(0) = B_{\theta 0}. \tag{15}$$

Finally, the charge conservation equation is written as

$$\frac{\partial \mathscr{R}}{\partial t} + \operatorname{div} \mathbf{J}_m = 0. \tag{16}$$

By also introducing $\mathbf{B}_m = (B_r, B_z)$ the meridian components of $\mathscr{B}$ and E_θ (resp., J_θ) the azimuthal component of $\mathscr{E}$ (resp., $\mathscr{J}$), the second system of unknowns $(E_\theta, \mathbf{B}_m)$ is written as

$$\begin{cases} \frac{\partial E_\theta}{\partial t} - c^2 \operatorname{curl} \mathbf{B}_m = -\frac{1}{\varepsilon_0} J_\theta, \\ \frac{\partial \mathbf{B}_m}{\partial t} + \operatorname{curl} E_\theta = 0, \\ \operatorname{div} \mathbf{B}_m = 0, \end{cases} \tag{17}$$

with the perfect conductor boundary conditions

$$\mathbf{B}_m \cdot \boldsymbol{\nu} = 0, \quad E_\theta = 0 \qquad \text{on } \gamma_b, \tag{18}$$

and the symmetry conditions on the axis γ_a

$$\mathbf{B}_m \cdot \boldsymbol{\nu} = B_r = 0, \quad E_\theta = 0 \qquad \text{on } \gamma_a. \tag{19}$$

For the initial conditions, we have

$$\mathbf{B}_m(0) = \mathbf{B}_{m0}, \quad E_\theta(0) = E_{\theta 0}. \tag{20}$$

For this system, there is no charge conservation equation.

2.3. A variational formulation

Both systems can be equivalently formulated as systems of second order in time. In the first one, the Ampère equation (1) and the Faraday equation (2) can be written as

$$\frac{\partial^2 \mathbf{E}_m}{\partial t^2} + c^2 \operatorname{curl}\operatorname{curl} \mathbf{E}_m = -\frac{1}{\varepsilon_0}\frac{\partial \mathbf{J}_m}{\partial t}, \tag{21}$$

$$\frac{\partial^2 B_\theta}{\partial t^2} + c^2 \operatorname{curl}\operatorname{curl} B_\theta = \frac{1}{\varepsilon_0}\operatorname{curl} \mathbf{J}_m, \tag{22}$$

whereas in the second one, one obtains

$$\frac{\partial^2 E_\theta}{\partial t^2} + c^2 \operatorname{curl}\operatorname{curl} E_\theta = -\frac{1}{\varepsilon_0}\frac{\partial J_\theta}{\partial t}, \tag{23}$$

$$\frac{\partial^2 \mathbf{B}_m}{\partial t^2} + c^2 \operatorname{curl}\operatorname{curl} \mathbf{B}_m = \frac{1}{\varepsilon_0}\operatorname{curl} J_\theta, \tag{24}$$

the other equations, boundary or initial conditions being unchanged. In addition, each of these second order in time systems has to be closed with a supplementary initial condition. Namely

$$\frac{\partial \mathbf{E}_m}{\partial t}(0) = c^2 \operatorname{curl} B_{\theta 0} - \frac{1}{\varepsilon_0}\mathbf{J}_m(0), \qquad \frac{\partial B_\theta}{\partial t}(0) = -\operatorname{curl} \mathbf{E}_{m0},$$

for the first one, and

$$\frac{\partial E_\theta}{\partial t}(0) = c^2 \operatorname{curl} \mathbf{B}_{m0} - \frac{1}{\varepsilon_0} J_\theta(0), \quad \frac{\partial \mathbf{B}_m}{\partial t}(0) = -\operatorname{curl} E_{\theta 0},$$

for the second one.

We now introduce a variational formulation of these problems, which can be applied independently of the (non) convexity of ω. Recall first that, to obtain control on the divergence of the fields, we have developed a method where the Maxwell equations are reformulated as a constrained problem, with associated Lagrange multipliers [5]. We thus set ϕ the Lagrange multiplier of the constraint $\operatorname{div} \mathbf{E}_m = \mathscr{R}/\varepsilon_0$ and ψ the Lagrange multiplier associated to $\operatorname{div} \mathbf{B}_m = 0$.

Let us define now the following functional spaces:

$$L^2_r(\omega) = \left\{ f : \omega \to \mathbb{R}; \int_\omega f^2 r \,\mathrm{d}r\,\mathrm{d}z < +\infty \right\}, \quad \|f\|_{0,\omega} = \left(\int_\omega f^2 r \,\mathrm{d}r\,\mathrm{d}z \right)^{1/2},$$

$$H^1_r(\omega) = \left\{ f \in L^2_r(\omega); \int_\omega |\mathrm{grad}\, f|^2 r \,\mathrm{d}r\,\mathrm{d}z < +\infty \right\}, \quad \|f\|_{1,\omega} = (\|f\|^2_{0,\omega} + \|\mathrm{grad}\, f\|^2_{0,\omega})^{1/2},$$

$$H^1_m(\omega) = \left\{ f \in H^1_r(\omega); \int_\omega \frac{f^2}{r} \,\mathrm{d}r\,\mathrm{d}z < +\infty \right\}, \quad \|f\|_{m,\omega} = \left(\|f\|^2_{1,\omega} + \|\frac{f}{r}\|^2_{0,\omega} \right)^{1/2},$$

$$H^1_{m0}(\omega) = \{ f \in H^1_m(\omega);\ f = 0 \text{ on } \gamma_b \}.$$

This allows to define the usual vector Sobolev spaces

$$\mathbf{L}^2_r(\omega) = L^2_r(\omega) \times L^2_r(\omega),$$

$$\mathbf{H}^1(\omega) = \{ \mathbf{v} = (v_r, v_z) \in \mathbf{L}^2_r(\omega);\ v_r \in H^1_m(\omega) \text{ and } v_z \in H^1_r(\omega) \}$$

and the classical spaces for the Maxwell equations

$$\mathbf{H}(\mathrm{curl}, \omega) = \{ \mathbf{v} \in \mathbf{L}^2_r(\omega);\ \mathrm{curl}\, \mathbf{v} \in \mathbf{L}^2_r(\omega) \}, \quad \mathbf{H}(\mathrm{div}, \omega) = \{ \mathbf{v} \in \mathbf{L}^2_r(\omega);\ \mathrm{div}\, \mathbf{v} \in L^2_r(\omega) \}.$$

This allows to define the corresponding subspaces with the vanishing tangential trace $\mathbf{H}_0(\mathrm{curl}, \omega)$ and normal trace $\mathbf{H}_0(\mathrm{div}, \omega)$, and finally the spaces of solutions

$$\mathbf{X} := \mathbf{H}_0(\mathrm{curl}, \omega) \cap \mathbf{H}(\mathrm{div}, \omega), \quad \mathbf{Y} := \mathbf{H}(\mathrm{curl}, \omega) \cap \mathbf{H}_0(\mathrm{div}, \omega)$$

endowed with the norms $\|\mathbf{v}\|_{\mathbf{X}} = \|\mathbf{v}\|_{\mathbf{Y}} = (\|\mathrm{curl}\, \mathbf{v}\|^2_{0,\omega} + \|\mathrm{div}\, \mathbf{v}\|^2_{0,\omega})^{1/2}$.

From now on, in the rest of this paper, we drop the subscripts m and θ for meridian and azimuthal fields, respectively (for instance $\mathbf{E}$ instead of $\mathbf{E}_m$, B instead of B_θ, etc.), since there is no ambiguity. Hence, the system (12) can be written in the following variational form:

Find $(\mathbf{E}, B, \phi) \in \mathbf{X} \times H^1_m(\omega) \times L^2_r(\omega)$ *such that*

$$\int_\omega \frac{\partial^2 \mathbf{E}}{\partial t^2} \cdot \mathbf{F} r \,\mathrm{d}r\,\mathrm{d}z + c^2 \int_\omega \mathrm{curl}\, \mathbf{E}\, \mathrm{curl}\, \mathbf{F} r \,\mathrm{d}r\,\mathrm{d}z + \int_\omega \phi\, \mathrm{div}\, \mathbf{F} r \,\mathrm{d}r\,\mathrm{d}z = -\frac{1}{\varepsilon_0} \int_\omega \frac{\partial \mathbf{J}}{\partial t} \cdot \mathbf{F} r \,\mathrm{d}r\,\mathrm{d}z \quad \forall \mathbf{F} \in \mathbf{X}, \tag{25}$$

$$\int_\omega \frac{\partial^2 B}{\partial t^2} C r \,\mathrm{d}r\,\mathrm{d}z + c^2 \int_\omega \mathrm{curl}\, B \cdot \mathrm{curl}\, C r \,\mathrm{d}r\,\mathrm{d}z = \frac{1}{\varepsilon_0} \int_\omega \mathbf{J} \cdot \mathrm{curl}\, C r \,\mathrm{d}r\,\mathrm{d}z \quad \forall C \in H^1_m(\omega), \tag{26}$$

$$\int_\omega \mathrm{div}\, \mathbf{E} q r \,\mathrm{d}r\,\mathrm{d}z = \frac{1}{\varepsilon_0} \int_\omega \mathscr{R} q r \,\mathrm{d}r\,\mathrm{d}z \quad \forall q \in L^2_r(\omega). \tag{27}$$

For the second system (17), one has, in a similar way

Find $(\mathbf{B}, E, \psi) \in \mathbf{Y} \times H^1_{m0}(\omega) \times L^2_r(\omega)$ *such that*

$$\int_\omega \frac{\partial^2 \mathbf{B}}{\partial t^2} \cdot \mathbf{C} r \,\mathrm{d}r\,\mathrm{d}z + c^2 \int_\omega \mathrm{curl}\, \mathbf{B}\, \mathrm{curl}\, \mathbf{C} r \,\mathrm{d}r\,\mathrm{d}z + \int_\omega \psi\, \mathrm{div}\, \mathbf{C} r \,\mathrm{d}r\,\mathrm{d}z = -\frac{1}{\varepsilon_0} \int_\omega J\, \mathrm{curl}\, \mathbf{C} r \,\mathrm{d}r\,\mathrm{d}z \quad \forall \mathbf{C} \in \mathbf{Y}, \tag{28}$$

$$\int_\omega \frac{\partial^2 E}{\partial t^2} Fr\,\mathrm{d}r\,\mathrm{d}z + c^2 \int_\omega \mathrm{curl}\,E \cdot \mathrm{curl}\,F\, r\,\mathrm{d}r\,\mathrm{d}z = -\frac{1}{\varepsilon_0}\int_\omega \frac{\partial J}{\partial t} Fr\,\mathrm{d}r\,\mathrm{d}z \quad \forall F \in H^1_{m0}(\omega), \tag{29}$$

$$\int_\omega \mathrm{div}\,\mathbf{B} qr\,\mathrm{d}r\,\mathrm{d}z = 0 \quad \forall q \in L^2_r(\omega). \tag{30}$$

Recall that the systems (25)–(27) and (28)–(30) are decoupled, cf. Section 2.2.

The azimuthal components (E, B), as the solution of a scalar wave equation, always belong to an H^1-style space, namely $H^1_m(\omega)$, even in a singular domain (see [3]), and an approximation by a P_1 Lagrange finite element method is well adapted. On the contrary, the meridian electric and magnetic fields $(\mathbf{E}, \mathbf{B})$ do not always belong to an H^1-style space as it would be automatically the case in a regular domain.

3. A decomposition in regular and singular parts

The underlying principle of the method consists in relating the singular solutions of Maxwell equations to those of the Laplace problem, the properties of the latter having been investigated in a detailed manner [3]. Let us briefly recall, without proof, some useful results in order to understand the construction of the numerical method [3].

We introduce the "regularized" spaces of solutions

$$\mathbf{X}_\mathrm{R} := \mathbf{X} \cap \mathbf{H}^1(\omega) \quad \text{and} \quad \mathbf{Y}_\mathrm{R} := \mathbf{Y} \cap \mathbf{H}^1(\omega).$$

These are the natural spaces of solutions in a regular domain. From the following property

Proposition 3.1. *The regularized spaces* $\mathbf{X}_\mathrm{R}$ *and* $\mathbf{Y}_\mathrm{R}$ *are closed, respectively, within* $\mathbf{X}$ *and* $\mathbf{Y}$.

we can split these spaces as

$$\mathbf{X} = \mathbf{X}_\mathrm{R} \overset{\perp}{\oplus} \mathbf{X}_\mathrm{S} \quad \text{and} \quad \mathbf{Y} = \mathbf{Y}_\mathrm{R} \overset{\perp}{\oplus} \mathbf{Y}_\mathrm{S}, \tag{31}$$

where $\mathbf{X}_\mathrm{S}$ and $\mathbf{Y}_\mathrm{S}$ are the spaces of the singular elements. When the domain is singular, $\mathbf{X}_\mathrm{S} \neq \{\mathbf{0}\}$ and $\mathbf{Y}_\mathrm{S} \neq \{\mathbf{0}\}$. More precisely, let $\beta^\star$ be the solution to the following equation, which involves a Legendre function: $P_{1/2}(\cos\pi/\beta^\star) = 0$. Its value is $\beta^\star \simeq 1.3771$, or $(\pi/\beta^\star) \simeq 130^\circ 43'$, and we have (see [3] for a proof).

Proposition 3.2. *The spaces* $\mathbf{X}_\mathrm{S}$ *and* $\mathbf{Y}_\mathrm{S}$ *are of finite dimension, namely*

$$\dim \mathbf{X}_\mathrm{S} = N_\mathrm{E} = \textit{number of conical points with vertex angle} > \frac{\pi}{\beta^\star} + \textit{number of reentrant edges},$$

$$\dim \mathbf{Y}_\mathrm{S} = N_\mathrm{B} = \textit{number of reentrant edges}. \tag{32}$$

By introducing now $(\mathbf{x}^i_\mathrm{S})_{i=1,N_\mathrm{E}}$ and $(\mathbf{y}^j_\mathrm{S})_{j=1,N_\mathrm{B}}$ the bases of $\mathbf{X}_\mathrm{S}$ and $\mathbf{Y}_\mathrm{S}$, the meridian electromagnetic fields solution of the Maxwell equations can be decomposed into

$$\mathbf{E}(t) = \mathbf{E}_\mathrm{R}(t) + \sum_{i=1}^{N_\mathrm{E}} \kappa^i(t)\mathbf{x}^i_\mathrm{S}, \tag{33}$$

$$\mathbf{B}(t) = \mathbf{B}_{\mathrm{R}}(t) + \sum_{j=1}^{N_{\mathrm{B}}} \delta^j(t)\mathbf{y}_{\mathrm{S}}^j, \tag{34}$$

where $(\kappa^i)_{i=1,N_{\mathrm{E}}}$ and $(\delta^j)_{j=1,N_{\mathrm{B}}}$ are smooth functions in time (at least continuous, cf. [3]).

We have now to characterize the singular parts on one hand, and the regular ones on the other.

3.1. A characterization of singular fields

This section describes the relationship between the singular electric and magnetic fields and the scalar singularities of Laplace-like operators. As it is proved in [3], other decompositions in regular and singular parts are possible, and can be better adapted to computations than (31). For instance, in the magnetic case, the divergence-free condition on the magnetic field allows us to use the *natural subspace* $\mathbf{W}$ of $\mathbf{Y}$ defined hereafter. For similar reasons, it is more convenient for the electric field to use another decomposition of the space $\mathbf{X}$, as we will see in the following.

3.1.1. Magnetic case

Due to the divergence-free condition on the magnetic field, let us now introduce the subspace $\mathbf{W}$ of $\mathbf{Y}$ as

$$\mathbf{W} = \{\mathbf{w} \in \mathbf{Y} : \operatorname{div} \mathbf{w} = 0\}, \quad \text{with norm } ||\operatorname{curl} \mathbf{w}||_{0,\omega}. \tag{35}$$

Then, if we define $\mathbf{W}_{\mathrm{R}} = \mathbf{W} \cap \mathbf{H}^1(\omega)$ the space of regular (divergence-free) fields, we proved in [2] that $\mathbf{W}_{\mathrm{R}}$ is closed in $\mathbf{W}$. Let $\mathbf{W}_{\mathrm{S}}$ be its orthogonal, i.e.

$$\mathbf{W} = \mathbf{W}_{\mathrm{R}} \overset{\perp}{\oplus} \mathbf{W}_{\mathrm{S}}. \tag{36}$$

The dimension of $\mathbf{W}_{\mathrm{S}}$ is also N_{B}, and any $\mathbf{w}_{\mathrm{S}} \in \mathbf{W}_{\mathrm{S}}$ is a *meridian* field that can be characterized as the solution to

$$\operatorname{curl} \mathbf{w}_{\mathrm{S}} = P_{\mathrm{S}} \quad \text{in } \omega, \tag{37}$$

$$\operatorname{div} \mathbf{w}_{\mathrm{S}} = 0 \quad \text{in } \omega, \tag{38}$$

$$\mathbf{w}_{\mathrm{S}} \cdot \boldsymbol{\nu} = 0 \quad \text{on } \gamma. \tag{39}$$

Here, P_{S} is a function that belongs to $L^2_r(\omega)$, but not to $H^1_r(\omega)$ or $H^1_m(\omega)$, such that

$$\Delta' P_{\mathrm{S}} = 0 \quad \text{in } \omega, \tag{40}$$

$$P_{\mathrm{S}} = 0 \quad \text{on } \gamma, \tag{41}$$

where the Laplace-like operator Δ' is defined as

$$\Delta' P_{\mathrm{S}} := \frac{\partial^2 P_{\mathrm{S}}}{\partial r^2} + \frac{\partial^2 P_{\mathrm{S}}}{\partial z^2} + \frac{1}{r}\frac{\partial P_{\mathrm{S}}}{\partial r} - \frac{P_{\mathrm{S}}}{r^2}. \tag{42}$$

3.1.2. Electric case

Except in the particular case of a charge-free problem, the electric field does not satisfy a divergence-free condition. Contrary to the magnetic case, it is not so fruitful to consider here the divergence-free subspace of $\mathbf{X}$. Moreover, both the reentrant edges *and* the conical points with a sufficient large vertex angle

contribute to the singular part of the solution as well. This increases the difficulty to compute (but not to characterize) the singular fields.

Under these circumstances, it is better to relax the orthogonality of the decomposition (31), by choosing singular fields $\mathbf{v}_S$ such that $\operatorname{curl}\mathbf{v}_S = 0$, in order to ease the computation of the singular fields. Instead of the decomposition of Proposition 3.2, we should rather use the (non-orthogonal) decomposition

$$\mathbf{X} = \mathbf{X}_R \oplus \operatorname{grad}\Phi_S, \tag{43}$$

where we denote by Φ_S the space of the *primal* singularities of the Laplacian, i.e., solutions of a Laplace problem that belong to $H^1_r(\omega)$ but lack an H^2-style regularity. More precisely, $\phi_S \in \Phi_S$ is characterized by the system

$$-\Delta\phi_S = p_S \quad \text{in } \omega, \tag{44}$$

$$\phi_S = 0 \quad \text{on } \gamma_b, \tag{45}$$

$$\frac{\partial\phi_S}{\partial\nu} = 0 \quad \text{on } \gamma_a, \tag{46}$$

where Δ is the trace of the three-dimensional Laplace operator in the meridian half-plane, defined by (10). There remains now to specify the right-hand side p_S of Eq. (44), which is a scalar function of regularity L^2_r (and not H^1_r), satisfying the same equations as ϕ_S, namely

$$\Delta p_S = 0 \quad \text{in } \omega, \tag{47}$$

$$p_S = 0 \quad \text{on } \gamma_b, \tag{48}$$

$$\frac{\partial p_S}{\partial\nu} = 0 \quad \text{on } \gamma_a. \tag{49}$$

It is called a *dual* singularity of the Laplacian. Finally, it is sufficient to take

$$\mathbf{v}_S = -\operatorname{grad}\phi_S \text{ in } \omega, \tag{50}$$

which can be equivalently characterized by

$$\operatorname{curl}\mathbf{v}_S = 0 \quad \text{in } \omega, \tag{51}$$

$$\operatorname{div}\mathbf{v}_S = p_S \quad \text{in } \omega, \tag{52}$$

$$\mathbf{v}_S \cdot \boldsymbol{\tau} = 0 \quad \text{on } \gamma_b, \tag{53}$$

$$\mathbf{v}_S \cdot \boldsymbol{\nu} = 0 \quad \text{on } \gamma_a. \tag{54}$$

Remark 3.3. If one wants to keep the orthogonality (for the norm $\mathbf{v} \mapsto \{\|\operatorname{curl}\mathbf{v}\|^2_{0,\omega} + \|\operatorname{div}\mathbf{v}\|^2_{0,\omega}\}^{1/2}$), which is equivalent to the canonical norm), it is possible to orthogonalize the decomposition (43). Subtracting to $\mathbf{v}_S$ its orthogonal projection $\pi\mathbf{v}_S$ on $\mathbf{X}_R$, we define $\mathbf{x}_S$ by $\mathbf{x}_S = (\mathbb{I} - \pi)\mathbf{v}_S$, with

$$\operatorname{curl}\mathbf{x}_S = -\operatorname{curl}(\pi\mathbf{v}_S) \quad \text{in } \omega \quad (\text{since } \operatorname{curl}\mathbf{v}_S = 0),$$

$$\operatorname{div}\mathbf{x}_S = p_S - \operatorname{div}(\pi\mathbf{v}_S) \quad \text{in } \omega \quad (\text{since } \operatorname{div}\mathbf{v}_S = p_S),$$

and $\pi\mathbf{v}_S \in \mathbf{X}_R$ is such that $(\mathbf{v}_S - \pi\mathbf{v}_S, \mathbf{v})_{\mathbf{X}} = 0\ \forall \mathbf{v} \in \mathbf{X}_R$. This is no difficulty (see [16] for a similar approach).

3.2. A characterization of regular fields

We now present the finite element approximation we actually used (without SCM) in the case of regular domains, that is when $\mathbf{X} \equiv \mathbf{X}_R$ and $\mathbf{Y} \equiv \mathbf{Y}_R$. Indeed, in the case of singular domains, the characterization of the regular fields $\mathbf{E}_R$ and $\mathbf{B}_R$ is still derived from this finite element approximation. We just have to modify the right-hand sides where the singular fields $\mathbf{E}_S$ and $\mathbf{B}_S$ appear, and to add some singular equations (see (88)–(90)).

As can be expected, a first characterization of the regular fields $\mathbf{E}_R$ and $\mathbf{B}_R$ is obtained by writing the same variational formulations as (25)–(27) for $(\mathbf{E}_R, B, \phi)$, and as (28)–(30) for $(\mathbf{B}_R, E, \psi)$, where, in this case, $\mathbf{E} \equiv \mathbf{E}_R$ and $\mathbf{B} \equiv \mathbf{B}_R$.

Let us introduce now a second variational formulation whose form appears more appropriate for the numerical computation: the augmented Lagrangian formulation. As in [5], one can equivalently add the equation of divergence (27) in (25) for the $\mathbf{E}_R$ field, and (30) in (28) for the $\mathbf{B}_R$ field. Now taking into account the property (see [12] or [2], Corollary 4.8, for the following axisymmetric expression).

Proposition 3.4. *For any* $\mathbf{u}, \mathbf{v} \in \mathbf{X}_R$, *we have*

$$\int_\omega \operatorname{curl}\mathbf{u} \cdot \operatorname{curl}\mathbf{v}\, r\,\mathrm{d}r\,\mathrm{d}z + \int_\omega \operatorname{div}\mathbf{u} \operatorname{div}\mathbf{v}\, r\,\mathrm{d}r\,\mathrm{d}z = \int_\omega \nabla\mathbf{u} : \nabla\mathbf{v} r\,\mathrm{d}r\,\mathrm{d}z + \int_\gamma u_v v_v v_r\,\mathrm{d}\gamma, \tag{55}$$

where u_v *stands for* $\mathbf{u}\cdot\boldsymbol{\nu}$, v_r *denotes the radial component of the normal* $\boldsymbol{\nu}$, *and the double dots* : *are the contracted product of two* 2×2 *tensors. We obtain*

Find $(\mathbf{E}_R, B, \phi) \in \mathbf{X}_R \times H^1_m(\omega) \times L^2_r(\omega)$ *such that*

$$\int_\omega \frac{\partial^2 \mathbf{E}_R}{\partial t^2} \cdot \mathbf{F}_R r\,\mathrm{d}r\,\mathrm{d}z + c^2 \int_\omega \nabla\mathbf{E}_R : \nabla\mathbf{F}_R r\,\mathrm{d}r\,\mathrm{d}z + c^2 \int_\gamma \mathbf{E}_R \cdot \boldsymbol{\nu}\mathbf{F}_R \cdot \boldsymbol{\nu} v_r\,\mathrm{d}\gamma + \int_\omega \phi \operatorname{div}\mathbf{F}_R r\,\mathrm{d}r\,\mathrm{d}z$$
$$= -\frac{1}{\varepsilon_0}\int_\omega \frac{\partial \mathbf{J}}{\partial t} \cdot \mathbf{F}_R r\,\mathrm{d}r\,\mathrm{d}z + \frac{c^2}{\varepsilon_0}\int_\omega \mathscr{R}\operatorname{div}\mathbf{F}_R r\,\mathrm{d}r\,\mathrm{d}z \quad \forall \mathbf{F}_R \in \mathbf{X}_R, \tag{56}$$

$$\int_\omega \frac{\partial^2 B}{\partial t^2} C r\,\mathrm{d}r\,\mathrm{d}z + c^2 \int_\omega \operatorname{curl} B \cdot \operatorname{curl} C\, r\,\mathrm{d}r\,\mathrm{d}z = \frac{1}{\varepsilon_0}\int_\omega \mathbf{J} \cdot \operatorname{curl} C\, r\,\mathrm{d}r\,\mathrm{d}z \quad \forall C \in H^1_m(\omega), \tag{57}$$

$$\int_\omega \operatorname{div}\mathbf{E}_R q r\,\mathrm{d}r\,\mathrm{d}z = \frac{1}{\varepsilon_0}\int_\omega \mathscr{R} q r\,\mathrm{d}r\,\mathrm{d}z \quad \forall q \in L^2_r(\omega), \tag{58}$$

which characterizes the regular electric field.

We now turn to the regular magnetic field $\mathbf{B}_R$. First, using similar arguments as above, the augmented Lagrangian formulation can be written. Then, with the help of the analogous of (55) in $\mathbf{Y}_R$ (the term $\int_\gamma u_v v_v v_r\,\mathrm{d}\gamma$ is replaced by $\int_\gamma u_\theta v_\theta v_r\,\mathrm{d}\gamma$, cf. [2]), we obtain the variational formulation which characterizes the regular magnetic field.

4. The numerical method

Starting from the above decomposition, it is possible to build a method, which allows to compute numerically the solution: this is the *SCM*, that can be summarized in two steps:

1. *Determination of bases of the singular spaces*. We first compute an approximation of bases of the singular spaces by solving static problems. The computations are carried out only once as an initialization procedure.
2. *Solution to the time-dependent problems*. It will then be enough to couple a classical Finite Element formulation (which can be already available) for the regular parts, and a low-dimensional linear system, for the singular parts.

Remark 4.1. This *complement* method can be easily included into already existing codes, without the costly procedure of rewriting them entirely. Thus, it provides an extension of the range of a code to the case of singular domains, or it can improve the efficiency of a code that can already handle singular domains.

Those steps are enumerated in the following sections.

4.1. Magnetic case: determination of $\mathbf{w}_S$, a basis of $\mathbf{W}_S$

4.1.1. Principle of the method

For the sake of simplicity, let us assume that the number of reentrant edges is equal to 1. The method to compute $\mathbf{w}_S$ is based on the characterization of the previous section. The algorithm is as follows:

- *First step*. We look for P_S, a non-vanishing element of $L^2_r(\omega)$ solution to (40), (41).
- *Second step*. Our task is now to compute $\mathbf{w}_S$ which satisfies (37)–(39). With a Lagrange finite element method, it is more convenient to invert a Laplacian operator (i.e., Δ') than a rotational one (i.e., curl). For this reason, instead of using the direct solution to (37)–(39), we make use of the property (see [2]) that, to $\mathbf{w}_S \in \mathbf{W}_S$, there corresponds one and only one potential ψ_S in $H^1_m(\omega)$ such that

$$-\Delta'\psi_S = P_S \quad \text{in } \omega, \tag{59}$$

$$\psi_S = 0 \quad \text{on } \gamma. \tag{60}$$

Now, as ψ_S is sufficiently smooth, one can easily solve this problem with the help of a variational formulation. The computation of $\mathbf{w}_S \in \mathbf{W}_S$ then stems from the identity $\mathbf{w}_S = \operatorname{curl}\psi_S$.

4.1.2. A numerical solution obtained by "singular lifting"

In a two-dimensional Cartesian geometry, a method was proposed in [4] to compute P_S through a local analytical expression defined as a series. In an axisymmetric domain, such an expression is only available as a double series. This makes the use of this approach very difficult. The "singular lifting" approach uses the property that there exist bases of such singular complement spaces made of fields regular everywhere except near the geometrical singularities. So it is sufficient to know the most singular part of the singularities (called the *principal part*) in the neighborhood of the reentrant edges (cf. [18]).

In the neighborhood of the reentrant corner E of the meridian domain ω (see Fig. 2), that is near the reentrant edge of the axisymmetric domain Ω, the solution P_S can be split into

$$P_S = P^0_p + \tilde{P}^0, \quad P^0_p = \rho^{-\alpha}\sin(\alpha\phi), \quad \tilde{P}^0 \text{ of } H^1\text{-style regularity},$$

where (ρ, ϕ) denotes the local polar coordinates centered at the reentrant corner (see Fig. 2). The "singular lifting" method consists in solving the problem in $\tilde{P}^0$:

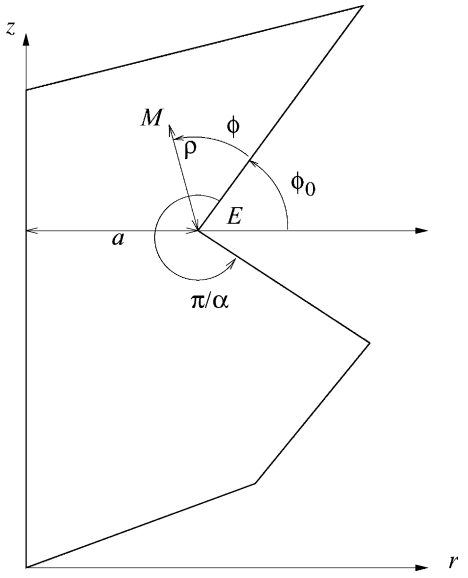

Fig. 2. Local coordinates near a reentrant corner.

Find $\tilde{P}^0$ *in the suitable space such that*

$$-\Delta'\tilde{P}^0 = \Delta' P_{\mathrm{p}}^0 \quad \text{in } \omega, \tag{61}$$

$$\tilde{P}^0_{|\gamma} = -P_{\mathrm{p}}^0 \quad \text{on } \gamma. \tag{62}$$

In most geometries (2D Cartesian or 3D polyhedral), the solution $\tilde{P}^0$ can be computed by a variational formulation. In those cases, it is justified by the following reasons:
1. The sufficient regularity of $\tilde{P}^0$.
2. The most singular terms of $\Delta' P_{\mathrm{p}}^0$ cancel, so that it belongs to H^{-1} (instead of H^{-2}).
3. P_{p}^0 has a vanishing trace on the two segments of γ that meet at the reentrant corner.

In the axisymmetric case however, there is a supplementary condition: P_{p}^0 has to be regular (i.e., H_m^1) near the z-axis, that is P_{p}^0 has to vanish near the z-axis. Unfortunately, P_{p}^0 does not fulfill such a requirement. A first remedy is to multiply P_{p}^0 by a regular cut-off function η, that is a regular function depending only on ρ such that $\eta \equiv 1$ near the reentrant corner and $\eta \equiv 0$ near the z-axis. Nevertheless, some numerical experiments (see for instance [16]) have shown that it is difficult to obtain good and robust numerical results by using a cut-off function, as this involves numerical instabilities well known for *singular function methods* (see for example [7]) and leads to high values of the constant in the error estimates. To overcome this difficulty, we actually use the following decomposition of P_{S}:

$$P_{\mathrm{S}} = P_{\mathrm{p}} + \tilde{P}, \quad P_{\mathrm{p}} = \frac{r}{a}\rho^{-\alpha}\sin(\alpha\phi), \tag{63}$$

where $\tilde{P}$ is a second function, which is regular *everywhere in* ω, i.e., $\tilde{P} \in H_m^1(\omega)$ and a denotes the distance between the reentrant corner and the the z-axis (see Fig. 2).

Remark 4.2.
1. The function r/a is nothing but the particular cut-off function that constrains the principal part to vanish on the z-axis (and not elsewhere).

2. Instead of multiplying $\rho^{-\alpha}\sin(\alpha\phi)$ by r/a, one could use the decomposition

$$P_S = (P_p^0(r,z) - P_p^0(0,z)) + \tilde{P}',$$

such that $\tilde{P}'$ is a regular variational solution of a problem similar to (64). But the corresponding right-hand side $\Delta'(P_p^0(r,z) - P_p^0(0,z))$ would be more difficult to handle.

First step: computation of P_S. The problem to solve reads

Find $\tilde{P} \in H^1_m(\omega)$ *such that*

$$-\Delta'\tilde{P} = \Delta' P_p = -\frac{3\alpha}{a}\rho^{-\alpha-1}\sin((\alpha+1)\phi+\phi_0) \quad \text{in } \omega, \tag{64}$$

$$\tilde{P}_{|\gamma} = -P_p \quad \text{on } \gamma, \tag{65}$$

which can be written in a variational form

$$\int_\omega \left\{ \operatorname{grad}\tilde{P}\cdot\operatorname{grad}\varphi + \frac{\tilde{P}\varphi}{r^2}\right\} r\,\mathrm{d}r\,\mathrm{d}z = -\int_\omega \Delta'\tilde{P}\varphi r\,\mathrm{d}r\,\mathrm{d}z$$
$$= -\frac{3\alpha}{a}\int_\omega \rho^{-\alpha-1}\sin((\alpha+1)\phi+\phi_0)\varphi r\,\mathrm{d}r\,\mathrm{d}z, \text{ where } \varphi \in H^1_{m0}(\omega). \tag{66}$$

The problem (66) is well posed.

In order to solve it numerically, a triangular mesh of ω is provided, and the space of solutions is discretized with the help of P_1 Lagrange Finite Elements. Let V_h be the space of H^1-conforming Finite Element functions thus generated, and let $\tilde{P}_h$ be the associated discrete solution. It can be written in the form $\tilde{P}_h = \sum_{i=1}^{N_h} P_i\lambda_i$, where $(\lambda_i)_{1\leqslant i\leqslant N_h}$ are the basis functions of V_h. After the discretization, the variational formulation (66) can be written as a linear system:

$$\mathbb{K}\vec{\mathsf{P}} = \vec{\mathsf{B}}, \tag{67}$$

with $\mathbb{K}$ a stiffness matrix suitably modified at the Dirichlet nodes, $\vec{\mathsf{P}}$ the vector of $\mathbb{R}^{N_h}$ of entries $(P_j)_j$, and $\vec{\mathsf{B}}$ the vector of $\mathbb{R}^{N_h}$ obtained after the numerical integration of the right-hand side of (66).

Second step: computation of $\mathbf{w}_S$.

Computation of the potential ψ_S. As mentioned earlier on, $\mathbf{w}_S$ is computed via its scalar potential ψ_S. One solves first system (59), (60). As ψ_S belongs to $H^1_m(\omega)$, it can be numerically solved by the H^1-conforming Finite Element method previously used for $\tilde{P}$, without requiring any kind of extra singular function. Nevertheless, the computation of $\mathbf{w}_S$ will be then obtained (in the following step) by applying the curl operator. This cannot be obtained via an H^1-conforming method, due to the singularity of $\mathbf{w}_S$. For this reason, we also use a decomposition of ψ_S in a regular and a singular part (similar to (63) for P_S), that is

$$\psi_S = \delta\psi_p + \tilde{\psi}, \psi_p = \frac{r}{a}\rho^\alpha\sin(\alpha\phi), \tag{68}$$

where the regular part $\tilde{\psi}$ is of H^2-style regularity and δ is a constant to be determined. Following [19], one can obtain an exact expression for the constant δ,

$$\delta = \frac{1}{\pi a}\int_\omega P_S^2 r\,\mathrm{d}r\,\mathrm{d}z. \tag{69}$$

We then compute $\tilde{\psi}$ like $\tilde{P}$ in the previous paragraph. A good approximation of δ can easily be obtained without any mesh refinement, cf. [11].

Computation of $\mathbf{w}_S$. One simply gets $\mathbf{w}_S$ by applying the curl operator to ψ_S decomposed into regular and singular parts (see (68)), so we have

$$\mathbf{w}_S = \operatorname{curl}\tilde{\psi} + \delta \operatorname{curl}\psi_p \stackrel{\text{def}}{=} \tilde{\mathbf{w}} + \delta \mathbf{w}_p. \tag{70}$$

The singular part $\mathbf{w}_p$ is obtained analytically and reads

$$\mathbf{w}_p = \rho^{\alpha-1}\begin{pmatrix} -\alpha\frac{r}{a}\cos((\alpha-1)\phi - \phi_0) \\ \frac{2}{a}\rho\sin(\alpha\phi) + \alpha\frac{r}{a}\sin((\alpha-1)\phi - \phi_0) \end{pmatrix}. \tag{71}$$

The regular part $\tilde{\mathbf{w}}$ is variationally computed as the solution to

$$\int_\omega \tilde{\mathbf{w}}\cdot\boldsymbol{\varphi} r\,\mathrm{d}r\,\mathrm{d}r\,\mathrm{d}z = \int_\omega \operatorname{curl}\tilde{\psi}\cdot\boldsymbol{\varphi} r\,\mathrm{d}r\,\mathrm{d}r\,\mathrm{d}z \quad \forall\boldsymbol{\varphi} \text{ a vector test function.} \tag{72}$$

This leads to solve, after discretization, the following linear system

$$\begin{pmatrix} \mathbb{M} & 0 \\ 0 & \mathbb{M} \end{pmatrix}\vec{\mathbf{w}} = \mathbb{R}\vec{\psi}, \tag{73}$$

where $\mathbb{R}$ denotes the curl matrix associated to the term $\int_\omega \operatorname{curl}\tilde{\psi}\cdot\boldsymbol{\varphi} r\,\mathrm{d}r\,\mathrm{d}r\,\mathrm{d}z$, and $\vec{\mathbf{w}}$ stands for the vector of $\mathbb{R}^{2N_h}$ of scalar entries $(w_j)_j$ associated to

$$\tilde{\mathbf{w}}_h = \sum_{i=1}^{N_h}\begin{pmatrix} w_{2i-1} \\ w_{2i} \end{pmatrix}\lambda_i. \tag{74}$$

Remark 4.3. The "singular lifting" method only requires the knowledge of the principal part of the singular function. Moreover its implementation is still rather straightforward in the case of several reentrant corners.

4.2. Electric case: determination of $\boldsymbol{v}_S$, a basis of grad Φ_S

4.2.1. Principle of the method

In this case, recall that there exist two kinds of geometrical singularities: the reentrant edges and the conical vertices with a sufficiently great vertex angle. Both cases will be treated in parallel, and only major differences will be detailed. Here again, for the sake of simplicity, we consider a domain ω with only one reentrant edge and one conical point of vertex angle $(\pi/\beta) > (\pi/\beta^{\star})$. How to compute $\mathbf{v}_S$ is based on the characterization (50). The framework of the algorithm is as follows:

- *First step*. We look for two non-vanishing elements p_S^e (for the edge) and p_S^c (for the conical point) that belong to $L^2_r(\omega)$ and satisfy (47)–(49).
- *Second step*. Our task is now to compute the singular basis elements $\mathbf{v}_S^e$ and $\mathbf{v}_S^c$, which satisfy (51)–(54) with p_S^e and p_S^c as respective right-hand sides. As for the magnetic case, it is more convenient to invert a Laplace operator Δ than a divergence operator div. Instead of using the direct solution to (51)–(54), we make use of the property (see [2]) that, to $\mathbf{v}_S^e$ and $\mathbf{v}_S^c$, there corresponds, respectively, one and only one potential ϕ_S^e and ϕ_S^c in $H^1_r(\omega)$ such that (44)–(46) is verified. Now, as these potentials are sufficiently smooth, one can easily solve these problems with the help of a variational formulation. The computation of $\mathbf{v}_S^e$ and $\mathbf{v}_S^c \in \operatorname{grad}\Phi_S$ then stems from the identities $\mathbf{v}_S^e = -\operatorname{grad}\phi_S^e$ and $\mathbf{v}_S^c = -\operatorname{grad}\phi_S^c$.

4.2.2. A numerical solution obtained by "singular lifting"

In the electric case, the numerical approach proposed in [4] could be used for the conical point, as local analytical expressions of p_S^c, ϕ_S^c and $\mathbf{v}_S^c$ as a series are available (see [3]). However, like in the magnetic case, such expressions are available only as a double series for the edge singularity. Moreover, the easiness of implementation of the singular lifting method led us to prefer this approach for both conical point and edge singularities.

In the neighborhood of the reentrant corner and of the conical point (with superscript e and c, respectively), the solution of the Δ problem can be split into

$$p_S^e = p_p^e + \tilde{p}^e \quad \text{and} \quad p_S^c = p_p^c + \tilde{p}^c, \tag{75}$$

where the *principal parts* p_p^e and p_p^c are only in $L_r^2(\omega)$, and the remainders $\tilde{p}^e$ and $\tilde{p}^c$ are in $H_r^1(\omega)$.

For the reentrant corner, one has for p_p^e an expression similar to the magnetic case (in the same local polar coordinates (ρ, ϕ), see Fig. 2), that is

$$p_p^e = \rho^{-\alpha} \sin(\alpha\phi).$$

For the conical point, we introduce (see Fig. 3) new local polar coordinates (ρ, ϕ) centered at the conical point C, with the origin of ϕ on the z-axis.

One obtains for p_p^c the following local expression

$$p_p^c = \rho^{-1-\nu} P_\nu(\cos\phi),$$

where P_ν denotes the Legendre function of index ν and $\nu \in]0, 1/2[$ is given by $P_\nu(\cos(\pi/\beta)) = 0$.

Remark 4.4. Contrary to the magnetic case, the variable p is well adapted for a finite element discretisation. No problem occurs near the z-axis and multiplying by a well-chosen cut-off function is useless.

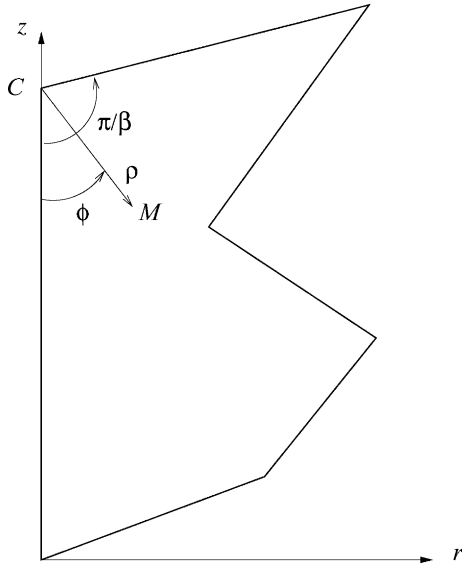

Fig. 3. Local coordinates near a reentrant conical point.

First step: *computation of* $p_{\mathrm{S}}^{\mathrm{e}}$ *and* $p_{\mathrm{S}}^{\mathrm{c}}$. Let us consider for example the computation of $p_{\mathrm{S}}^{\mathrm{c}}$. Let us use the decomposition (75) together with the property that $p_{\mathrm{p}}^{\mathrm{c}} = \rho^{-1-\nu}P_{\nu}(\cos\phi)$ verifies

$$\Delta p_{\mathrm{p}}^{\mathrm{c}} = 0,$$

$$\frac{\partial p_{\mathrm{p}}^{\mathrm{c}}}{\partial \nu} = 0 \quad \text{on } \gamma_a.$$

The problem to solve reads

Find $\tilde{p}^{\mathrm{c}} \in H_r^1(\omega)$ *such that*

$$-\Delta\tilde{p}^{\mathrm{c}} = 0 \quad \text{in } \omega, \tag{76}$$

$$\tilde{p}^{\mathrm{c}} = -p_{\mathrm{p}}^{\mathrm{c}} \quad \text{on } \gamma_b, \tag{77}$$

$$\frac{\partial\tilde{p}^{\mathrm{c}}}{\partial \nu} = 0 \quad \text{on } \gamma_a. \tag{78}$$

It can be written in the variational form, as previously, with the help of a suitable lifting of the trace $p_{p|\gamma_b}^{\mathrm{c}}$. In order to solve it numerically, Lagrange Finite Elements are used again. The variational formulation can be written, after discretization, as the following linear system:

$$\mathbb{K}^{\mathrm{c}}\vec{\mathsf{p}} = \vec{\mathsf{b}}, \tag{79}$$

with obvious notations.

Remark 4.5.

1. The non-homogeneous Dirichlet boundary condition only requires the computation of $\rho^{-1-\nu}P_{\nu}(\cos\phi)$ on the edges γ_k of the boundary γ_b, except for the one with an extremity on the conical point (i.e., $\phi = \pi/\beta$).
2. Note that the stiffness matrix $\mathbb{K}^{\mathrm{c}}$ is a part of the matrix $\mathbb{K}$ introduced for the magnetic case, which is an interesting property from a computational point of view.

The computation of $p_{\mathrm{S}}^{\mathrm{e}}$ is performed in the same way.

Second step: *computation of* $\mathbf{v}_{\mathrm{S}}^{\mathrm{e}}$ *and* $\mathbf{v}_{\mathrm{S}}^{\mathrm{c}}$.

Computation of the potentials $\phi_{\mathrm{S}}^{\mathrm{e}}$ *and* $\phi_{\mathrm{S}}^{\mathrm{c}}$. Here again, we expose the computation of $\phi_{\mathrm{S}}^{\mathrm{c}}$; $\phi_{\mathrm{S}}^{\mathrm{e}}$ can be obtained in a similar way. As mentioned earlier on, $\mathbf{v}_{\mathrm{S}}^{\mathrm{c}}$ is computed via its scalar potential $\phi_{\mathrm{S}}^{\mathrm{c}}$. One solves first the system (44)–(46). As $\phi_{\mathrm{S}}^{\mathrm{c}} \in H_r^1(\omega)$, it could be numerically solved by the H^1-conforming Finite Element method previously used for $\tilde{p}^{\mathrm{c}}$, without requiring any kind of extra singular function. Nevertheless, the computation of $\mathbf{v}_{\mathrm{S}}^{\mathrm{c}}$ would then be obtained (in the following step) by applying the grad operator, which cannot be made by a H^1-conforming method, due to the singularity of $\mathbf{v}_{\mathrm{S}}^{\mathrm{c}}$. For this reason, we prefer to use a decomposition of $\phi_{\mathrm{S}}^{\mathrm{c}}$ in a regular and a singular part, that is

$$\phi_{\mathrm{S}}^{\mathrm{c}} = \delta^{\mathrm{c}}\phi_{\mathrm{p}}^{\mathrm{c}} + \tilde{\phi}^{\mathrm{c}}, \quad \phi_{\mathrm{p}}^{\mathrm{c}} = \rho^{\nu}P_{\nu}(\cos\phi), \tag{80}$$

where the regular part $\tilde{\phi}^{\mathrm{c}}$ is of H^2-style regularity and δ^{c} is the singular coefficient which can be evaluated (for instance as in [19]) to obtain

$$\delta^{\mathrm{c}} = \frac{\int_{\omega}(p_{\mathrm{p}}^{\mathrm{c}})^2 r\,\mathrm{d}r\,\mathrm{d}z}{(1+2\nu)\int_0^{\pi/\beta}(P_{\nu}(\cos\phi))^2\sin\phi\,\mathrm{d}\phi}. \tag{81}$$

We then compute $\tilde{\phi}^{\mathrm{c}}$ as we did for $\tilde{\psi}$ in the magnetic case.

Computation of $\mathbf{v}_{\mathrm{S}}^{\mathrm{e}}$ *and* $\mathbf{v}_{\mathrm{S}}^{\mathrm{c}}$. One simply gets $\mathbf{v}_{\mathrm{S}}^{\mathrm{e}}$ and $\mathbf{v}_{\mathrm{S}}^{\mathrm{c}}$ by applying the $-\mathrm{grad}$ operator to $\phi_{\mathrm{S}}^{\mathrm{e}}$ and to $\phi_{\mathrm{S}}^{\mathrm{c}}$, respectively, decomposed into regular and singular parts. So we have

$$\mathbf{v}_{\mathrm{S}}^{\mathrm{e}} = -\mathrm{grad}\,\tilde{\phi}^{\mathrm{e}} - \delta^{\mathrm{e}}\mathrm{grad}\,\phi_{\mathrm{p}}^{\mathrm{e}} \stackrel{\mathrm{def}}{=} \tilde{\mathbf{v}}^{\mathrm{e}} + \delta^{\mathrm{e}}\mathbf{v}_{\mathrm{p}}^{\mathrm{e}}, \tag{82}$$

$$\mathbf{v}_{\mathrm{S}}^{\mathrm{c}} = -\mathrm{grad}\,\tilde{\phi}^{\mathrm{c}} - \delta^{\mathrm{c}}\mathrm{grad}\,\phi_{\mathrm{p}}^{\mathrm{c}} \stackrel{\mathrm{def}}{=} \tilde{\mathbf{v}}^{\mathrm{c}} + \delta^{\mathrm{c}}\mathbf{v}_{\mathrm{p}}^{\mathrm{c}}. \tag{83}$$

The singular parts $\mathbf{v}_{\mathrm{p}}^{\mathrm{e}}$ and $\mathbf{v}_{\mathrm{p}}^{\mathrm{c}}$ are obtained analytically and read

$$\mathbf{v}_{\mathrm{p}}^{\mathrm{e}} = \alpha\rho^{\alpha-1}\begin{pmatrix} \frac{1}{r}\sin((\alpha-1)\phi-\phi_0) \\ \cos((\alpha-1)\phi-\phi_0) \end{pmatrix}, \tag{84}$$

$$\mathbf{v}_{\mathrm{p}}^{\mathrm{c}} = \nu\rho^{\nu-1}\begin{pmatrix} P_\nu(\cos\phi)\cos\phi - P_\nu^1(\cos\phi)\sin\phi \\ P_\nu(\cos\phi)\sin\phi + P_\nu^1(\cos\phi)\cos\phi \end{pmatrix}. \tag{85}$$

The regular part $\tilde{\mathbf{v}}^{\mathrm{e}}$ is variationally computed as the solution to

$$\int_\omega \tilde{\mathbf{v}}^{\mathrm{e}}\cdot\boldsymbol{\varphi} r\,\mathrm{d}r\,\mathrm{d}z = -\int_\omega \mathrm{grad}\,\tilde{\phi}^{\mathrm{e}}\cdot\boldsymbol{\varphi} r\,\mathrm{d}r\,\mathrm{d}z \quad \forall \text{ vector test function } \boldsymbol{\varphi}. \tag{86}$$

After discretization, that leads to solve the following linear system:

$$\begin{pmatrix} \mathbb{M} & 0 \\ 0 & \mathbb{M} \end{pmatrix}\vec{\tilde{\mathbf{v}}}^{\mathrm{e}} = -\mathbb{G}\vec{\phi}^{\mathrm{e}}. \tag{87}$$

Above, $\mathbb{G}$ denotes the gradient matrix associated to the term $\int_\omega \mathrm{grad}\,\tilde{\phi}^{\mathrm{e}}\cdot\boldsymbol{\varphi} r\,\mathrm{d}r\,\mathrm{d}z$, and $\vec{\tilde{\mathbf{v}}}^{\mathrm{e}}$ stands for the vector of $\mathbb{R}^{2N_h}$ of entries $(v_j^{\mathrm{e}})_j$ defined like in (74).

One can use a similar variational formulation and perform the same discretization for $\tilde{\mathbf{v}}^{\mathrm{c}}$. This is no difficulty.

4.3. Solution to the time-dependent problem

In what follows, we focus on the electric field formulation. Indeed, contrary to the magnetic case, the electric field does not satisfy (in general) the divergence-free condition and the coupling between the regular and the singular part of the solution is "stronger". For the divergence-free magnetic field, there is no difficulty to write the formulation. It can be easily deduced from the electric one or from the one presented in [4] for a Cartesian geometry (also in a divergence-free case).

A new variational formulation of the problem (25) and (27) is introduced (we do not consider the computation of B which is regular), using the (non-orthogonal) decomposition of the space $\mathbf{X} = \mathbf{X}_{\mathrm{R}} \oplus \mathrm{grad}\,\Phi_{\mathrm{S}}$, and of the solution $\mathbf{E}(t) = \mathbf{E}_{\mathrm{R}}(t) + \sum_{i=1}^{N_{\mathrm{E}}}\kappa^i(t)\mathbf{v}_{\mathrm{S}}^i$. We add to the space of test functions $\mathbf{X}_{\mathrm{R}}$ the functions $(\mathbf{v}_{\mathrm{S}}^i)_{i=1,N_{\mathrm{E}}}$. With this decomposition, the variational formulation (25) and (27) becomes

Find $(\mathbf{E}_{\mathrm{R}}, \boldsymbol{\kappa}, \phi) \in \mathbf{X}_{\mathrm{R}} \times \mathbb{R}^{N_{\mathrm{E}}} \times L^2_r(\omega)$ *such that*

$$\begin{aligned} &\int_\omega \frac{\partial^2\mathbf{E}_{\mathrm{R}}}{\partial t^2}\cdot\mathbf{F}_{\mathrm{R}} r\,\mathrm{d}r\,\mathrm{d}z + \sum_{i=1}^{N_{\mathrm{E}}}(\kappa^i)''\int_\omega \mathbf{v}_{\mathrm{S}}^i\cdot\mathbf{F}_{\mathrm{R}} r\,\mathrm{d}r\,\mathrm{d}z + c^2\int_\omega \nabla\mathbf{E}_{\mathrm{R}} : \nabla\mathbf{F}_{\mathrm{R}} r\,\mathrm{d}r\,\mathrm{d}z + c^2\int_\gamma \mathbf{E}_{\mathrm{R}}\cdot\boldsymbol{\nu}\mathbf{F}_{\mathrm{R}}\cdot\boldsymbol{\nu} v_r\,\mathrm{d}\gamma \\ &\quad + \int_\omega \phi\,\mathrm{div}\,\mathbf{F}_{\mathrm{R}} r\,\mathrm{d}r\,\mathrm{d}z = -\frac{1}{\varepsilon_0}\int_\omega \frac{\partial\mathbf{J}}{\partial t}\cdot\mathbf{F}_{\mathrm{R}} r\,\mathrm{d}r\,\mathrm{d}z + \frac{c^2}{\varepsilon_0}\int_\omega \mathscr{R}\mathrm{div}\,\mathbf{F}_{\mathrm{R}} r\,\mathrm{d}r\,\mathrm{d}z \quad \forall\mathbf{F}_{\mathrm{R}} \in \mathbf{X}_{\mathrm{R}}, \end{aligned} \tag{88}$$

$$\int_\omega \operatorname{div} \mathbf{E}_{\mathrm{R}} q r \,\mathrm{d}r\,\mathrm{d}z + \sum_{i=1}^{N_{\mathrm{E}}} \kappa^i \int_\omega \operatorname{div} \mathbf{v}_{\mathrm{S}}^i q r \,\mathrm{d}r\,\mathrm{d}z = \frac{1}{\varepsilon_0} \int_\omega \mathscr{R} q r \,\mathrm{d}r\,\mathrm{d}z \quad \forall q \in L^2_r(\omega), \tag{89}$$

supplemented with the N_{E} additional equations, obtained by taking $(\mathbf{v}_{\mathrm{S}}^i)_{1 \leqslant i \leqslant N_{\mathrm{E}}}$ as test functions. One gets

$$\int_\omega \frac{\partial^2 \mathbf{E}_{\mathrm{R}}}{\partial t^2} \cdot \mathbf{v}_{\mathrm{S}}^j r \,\mathrm{d}r\,\mathrm{d}z + \sum_{i=1}^{N_{\mathrm{E}}} (\kappa^i)'' \int_\omega \mathbf{v}_{\mathrm{S}}^i \cdot \mathbf{v}_{\mathrm{S}}^j r \,\mathrm{d}r\,\mathrm{d}z + \int_\omega \phi \operatorname{div} \mathbf{v}_{\mathrm{S}}^j r \,\mathrm{d}r\,\mathrm{d}z = -\frac{1}{\varepsilon_0} \int_\omega \frac{\partial \mathbf{J}}{\partial t} \cdot \mathbf{v}_{\mathrm{S}}^j r \,\mathrm{d}r\,\mathrm{d}z, \quad 1 \leqslant j \leqslant N_{\mathrm{E}}. \tag{90}$$

Above, $(\kappa^i)''$ denote the second derivative of $\kappa^i(t)$ with respect to the time variable. The set of equations (88)–(90) is the system we now have to solve, to be compared to (56) and (58) in the case of a regular domain.

Starting from the variational mixed formulation (88)–(90), we are now ready to derive a Finite Element + Singular Complement approximation. Let $\mathbf{X}_{\mathrm{R}}^h \subset \mathbf{X}_{\mathrm{R}}$ and $Q^h \subset L^2_r(\omega)$ be the spaces of discretized test functions, that are chosen in such a way that the discrete inf-sup condition is satisfied [10]. Recall that we actually used the modified Taylor–Hood element. It leads to a diagonal mass matrix (i.e., the usual mass lumping, obtained by using an appropriate quadrature formula). This element requires the definition of two levels of meshes. A coarser triangulation of the domain ω is first defined, and then, a finer one is obtained by dividing each triangle K_{2h} into four subtriangles K_h of equal surface. Then, the approximation spaces for the vector fields is made of functions which are componentwise P_1-conforming on the finer triangulation. At the same time, the approximation space for the Lagrange multipliers consists of the P_1-conforming finite element on the coarser grid.

Let now $\mathbf{E}^h(t) = \mathbf{E}_{\mathrm{R}}^h(t) + \sum_{i=1}^{N_{\mathrm{E}}} \kappa^{h,i}(t) \mathbf{v}_{\mathrm{S}}^{h,i}$ be the discrete solution. Like in (74), one has

$$\mathbf{E}_{\mathrm{R}}^h(t) = \sum_{i=1}^{N_h} \begin{pmatrix} E_{R,2i-1}(t) \\ E_{R,2i}(t) \end{pmatrix} \lambda_i.$$

By using the same decomposition on each quantity defined on the finer or on the coarser mesh, the semi-discretized variational formulation is written (with the addition of the index h) in the same way as (88)–(90). It can be then written equivalently as the following linear system:

$$\frac{\mathrm{d}^2}{\mathrm{d}t^2} \mathbb{M}_\omega \vec{\mathbf{E}}_{\mathrm{R}} + \mathbb{M}_{rs} \vec{\kappa}'' + c^2 (\mathbb{K}_\omega + \mathbb{K}_\gamma) \vec{\mathbf{E}}_{\mathrm{R}} + \mathbb{L}_\omega \vec{\phi} = -\frac{1}{\varepsilon_0} \frac{\mathrm{d}}{\mathrm{d}t} \mathbb{M}_\omega \vec{\mathbf{J}} + \frac{c^2}{\varepsilon_0} \mathbb{L}_\omega \vec{\mathbf{R}}, \tag{91}$$

$$\frac{\mathrm{d}^2}{\mathrm{d}t^2} \mathbb{M}_{sr} \vec{\mathbf{E}}_{\mathrm{R}} + \mathbb{M}_s \vec{\kappa}'' + \mathbb{L}_s \vec{\phi} = -\frac{1}{\varepsilon_0} \frac{\mathrm{d}}{\mathrm{d}t} \mathbb{M}_{sr} \vec{\mathbf{J}}, \tag{92}$$

$${}^t\mathbb{L}_\omega \vec{\mathbf{E}}_{\mathrm{R}} + {}^t\mathbb{L}_s \vec{\kappa} = \frac{1}{\varepsilon_0} \mathbb{M}_\omega^{\mathrm{c}} \vec{\mathbf{R}}, \tag{93}$$

where $\mathbb{K}_\omega$ and $\mathbb{K}_\gamma$ denote the matrices associated to the terms $\int_\omega \nabla \mathbf{E}_{\mathrm{R}} : \nabla \mathbf{F}_{\mathrm{R}} r \,\mathrm{d}r\,\mathrm{d}z$ and $\int_\gamma \mathbf{E}_{\mathrm{R}} \cdot \boldsymbol{\nu} \mathbf{F}_{\mathrm{R}} \cdot \boldsymbol{\nu} \nu_r \,\mathrm{d}\gamma$, respectively, $\mathbb{L}_\omega$ denotes the matrix associated to the term $\int_\omega \phi \operatorname{div} \mathbf{F}_{\mathrm{R}} r \,\mathrm{d}r\,\mathrm{d}z$. The matrix $\mathbb{M}_{rs}$ is a rectangular one, coming from the integral over ω of the product of the N_{E} singular functions $\mathbf{v}_{\mathrm{S}}^i$ by the basis functions of $\mathbf{X}_{\mathrm{R}}^h$, and $\vec{\kappa}$ stands for the vector of $\mathbb{R}^{N_{\mathrm{E}}}$ of entries $\kappa^i(t)$. Then $\mathbb{M}_s$ is the "singular" mass matrix associated to the term $\int_\omega \mathbf{v}_{\mathrm{S}}^i \cdot \mathbf{v}_{\mathrm{S}}^j r \,\mathrm{d}r\,\mathrm{d}z$, and $\mathbb{L}_s$ the "singular gradient matrix" resulting from the discretization of $\int_\omega \operatorname{div} \mathbf{v}_{\mathrm{S}}^i q r \,\mathrm{d}r\,\mathrm{d}z$. Finally, $\mathbb{M}_{rs}$ is the transpose of $\mathbb{M}_{sr}$, and the superscript c recalls that the mass matrix $\mathbb{M}_\omega^{\mathrm{c}}$ is defined on the coarser mesh. For the singular matrices, the computation must be carried out precisely in the neighborhood of the reentrant corners. This point will be detailed in Section 4.4.

We then perform a time discretization involving a second-order explicit (leap-frog) scheme. Here the notation X^n (resp., X^{n+1}) stands for a variable X at time $t^n = n\Delta t$ (resp., $t^{n+1} = (n+1)\Delta t$), where Δt is the time-step. $\vec{\mathsf{F}}^n, \vec{\mathsf{G}}^n, \vec{\mathsf{H}}^n$ is the set of quantities known at time t^n for each equation of the scheme (91)–(93), which can be rewritten as

$$\mathbb{M}_\omega \vec{\mathsf{E}}_{\mathrm{R}}^{n+1} + \mathbb{M}_{rs}\vec{\kappa}^{n+1} + \mathbb{L}_\omega \vec{\phi}^{n+1} = \vec{\mathsf{F}}^n, \tag{94}$$

$$\mathbb{M}_{sr}\vec{\mathsf{E}}_{\mathrm{R}}^{n+1} + \mathbb{M}_s\vec{\kappa}^{n+1} + \mathbb{L}_s \vec{\phi}^{n+1} = \vec{\mathsf{G}}^n, \tag{95}$$

$${}^t\mathbb{L}_\omega \vec{\mathsf{E}}_{\mathrm{R}}^{n+1} + {}^t\mathbb{L}_s\vec{\kappa}^{n+1} = \vec{\mathsf{H}}^n. \tag{96}$$

To solve this linear system, a convenient way is to decouple $\vec{\kappa}^{n+1}$ and the unknowns $(\vec{\mathsf{E}}_{\mathrm{R}}^{n+1}, \vec{\phi}^{n+1})$. In [4], we proposed a solver based on the same idea, for a two-dimensional Cartesian divergence-free Maxwell system of equations, in the case of a single reentrant corner. The method we will develop here is more general, since it is well suited for a domain with several reentrant corners, and for a problem with a non-vanishing divergence.

Substituting (94) $-\mathbb{M}_{rs}\mathbb{M}_s^{-1}$ (95) for Eqs. (94) and (96)$-{}^t\mathbb{L}_s\mathbb{M}_s^{-1}$(95) for Eq. (96), we obtain a system where $\vec{\kappa}^{n+1}$ does no appear any more. It is written as (where the superscript $\sim$ denotes the quantities obtained after these algebraic manipulations)

$$\widetilde{\mathbb{M}}\vec{\mathsf{E}}_{\mathrm{R}}^{n+1} + \widetilde{\mathbb{L}}\vec{\phi}^{n+1} = \widetilde{\vec{\mathsf{F}}^n}, \tag{97}$$

$${}^t\widetilde{\mathbb{L}}\vec{\mathsf{E}}_{\mathrm{R}}^{n+1} + {}^t\mathbb{L}_s\mathbb{M}_s^{-1}\mathbb{L}_s\vec{\phi}^{n+1} = \widetilde{\vec{\mathsf{H}}^n}. \tag{98}$$

It remains now to invert this system. Following the idea we developed for regular domains (see [5]), this is achieved with the help of an Uzawa algorithm (see for instance [14]). Compared to the unmodified system – that is the system obtained in a regular domain – it requires essentially two modifications. The first one is the computation of the matrix $\mathbb{M}_s^{-1}$. $\mathbb{M}_s$ being a symmetric definite positive matrix (by construction) of dimension $N_{\mathrm{E}} \times N_{\mathrm{E}}$, i.e., a few units (and often $N_{\mathrm{E}} = 1$), $\mathbb{M}_s^{-1}$ is very easy to compute once and for all. The second one is concerned with the algebraic solver associated to $\widetilde{\mathbb{M}} \overset{\mathrm{def}}{=} \mathbb{M}_\omega - \mathbb{M}_{rs}\mathbb{M}_s^{-1}\mathbb{M}_{sr}$. It can be solved (for instance) with the help of the following formula (see [15] for a review),

$$(\mathbb{A} - \mathbb{U}\mathbb{V}^{\mathrm{T}})^{-1} = \mathbb{A}^{-1} + \mathbb{A}^{-1}\mathbb{U}(\mathbb{I} - \mathbb{V}^{\mathrm{T}}\mathbb{A}^{-1}\mathbb{U})^{-1}\mathbb{V}^{\mathrm{T}}\mathbb{A}^{-1}.$$

Above $\mathbb{A}$ is an $N \times N$ matrix and $\mathbb{U}$ and $\mathbb{V}$ are $N \times K$ matrices. This formula is particularly well adapted when $\mathbb{A}^{-1}$ is known. As a matter of fact, it only requires the additional computation of the small $K \times K$ matrix $(\mathbb{I} - \mathbb{V}^{\mathrm{T}}\mathbb{A}^{-1}\mathbb{U})^{-1}$. In our case, we have $\mathbb{A} \overset{\mathrm{def}}{=} \mathbb{M}_\omega$, $\mathbb{U} \overset{\mathrm{def}}{=} \mathbb{M}_{rs}$ and $\mathbb{V} \overset{\mathrm{def}}{=} \mathbb{M}_s^{-1}\mathbb{M}_{sr}$. Recall that the mass matrix $\mathbb{M}_\omega$ is diagonal, thanks to a quadrature formula (see [5]), which preserves the accuracy. Hence, it is easy to solve the linear system (97), (98), which now appears as a slight modification of the one obtained for the unmodified system.

Once the values of $(\vec{\mathsf{E}}_{\mathrm{R}}^{n+1}, \vec{\phi}^{n+1})$ are computed, one can also compute, at the corresponding time, the value $\vec{\kappa}^{n+1}$, by solving (95).

4.4. Some details concerning the numerical integration

To conclude this Section, let us briefly present some details concerning the numerical integration, especially in the two instances that deserve special attention.

The first one is the computation of the singular coefficients that appear in the matrices $\mathbb{M}_s$, $\mathbb{M}_{rs}$ or $\mathbb{L}_s$, and in the constants δ, δ^c (cf. (69), (81)).

For illustrative purposes, consider the term $\int_\omega P_S^2 r\,dr\,dz$ in (69). A convenient way to compute this integral is to use the decomposition (63) in a regular part $\tilde{P}$ and a singular one P_p:

$$\int_\omega P_S^2 r\,dr\,dz = \int_\omega (\tilde{P}+P_p)^2 r\,dr\,dz = \int_\omega \tilde{P}^2 r\,dr\,dz + 2\int_\omega \tilde{P}P_p r\,dr\,dz + \int_\omega P_p^2 r\,dr\,dz.$$

By using the discrete form $\tilde{P}_h = \sum_{i=1}^{N_h} P_i\lambda_i$ of $\tilde{P}$, and the analytical expression of P_p, we obtain

$$\sum_{i,j=1}^{N_h} P_iP_j \int_\omega \lambda_i\lambda_j r\,dr\,dz + 2\sum_{j=1}^{N_h} P_j \int_\omega P_p\lambda_j r\,dr\,dz + \frac{1}{a^2}\int_\omega \rho^{-2\alpha}(\sin(\alpha\phi))^2 r^3\,dr\,dz.$$

The first term is the product of the mass matrix by the vector of entries P_i and is straightforward to compute. The other two are singular (near a reentrant corner or conical point) and are computed thanks to a quadrature formula. Actually, we used a sixth-order Gauss–Hammer formula (see for instance [22]), with seven integration points located *inside* each triangle, that does not require the unbounded value of the singular part. The computation of the other singular coefficients is carried out along the same lines.

The second instance that deserves special care is the numerical evaluation of integrals of the form

$$\int_\omega \frac{u_\theta v_\theta}{r}\,dr\,dz. \tag{99}$$

These terms appear in the computation of azimuthal components B and E – see the integrals $\int_\omega \operatorname{curl} B\cdot\operatorname{curl} Cr\,dr\,dz$ in (26) and $\int_\omega \operatorname{curl} E\cdot\operatorname{curl} Fr\,dr\,dz$ in (29) – and also in the computation of the meridian components, if an augmented Lagrangian formulation is used. In the continuous case however, this is no difficulty since it is assumed that the functions and components u all belong to spaces such that $\int_\omega (u^2/r)\,dr\,dz < \infty$.

To compute (99), we have to derive in each triangle K_h the quadrature formula

$$\int_{K_h} \frac{uv}{r}\,dr\,dz = \sum_{\alpha=1}^{3}\sum_{\beta=1}^{3} w_{\alpha,\beta}u(a_\alpha)v(a_\beta)$$

for all $u\in P_1(K_h)$ and $v\in P_1(K_h)$, such that $u(a_\alpha)=v(a_\alpha)=0$ if the node a_α belongs to γ_a. The easiest way is to compute an *exact* formula, either by going back to the reference element $\hat{K}$, or by direct computations (integrate first in z, then in r).

If one considers a triangle with a single vertex a_1 on the axis γ_a, the weights $(w_{\alpha,\beta})_{\alpha,\beta=1,2,3}$ remain bounded in r_2, r_3, the r-coordinates of the other two nodes of the triangle K_h. If one considers a triangle with two vertices a_1, a_2 on the axis γ_a, the weights $(w_{\alpha,\beta})_{\alpha,\beta=1,2,3}$ are in $\log r_3$, with r_3 the r-coordinate of the third node of the triangle K_h.

As expected, in both cases, the behavior is balanced by the vanishing condition on γ_a, as the P_1 variables tend to 0 in the same way as (r_2, r_3) (resp., r_3).

5. The Silver–Müller boundary condition

Let us consider again the problem set in the three-dimensional domain Ω. We suppose that a perfectly conducting boundary condition is applied on a part Γ_C of the boundary ($\Gamma_C \subset \Gamma$) of the domain. The remaining part Γ_S is an artificial boundary, on which the interaction between the domain and the exterior is modeled. Here we have chosen the simple model, that is

$$\left(\mathscr{E} - c\mathscr{B} \times \mathbf{n}\right) \times \mathbf{n} = \mathscr{G} \times \mathbf{n} \quad \text{on } \Gamma_S, \tag{100}$$

where $\mathscr{G}$ is given. Now in the meridian domain ω, we denote by γ_S the intersection of Γ_S with the meridian half-plane, and this condition reads for the first system of unknowns $(\mathbf{E}, B)$

$$\mathbf{E} \cdot \boldsymbol{\tau} - cB = \mathbf{g} \cdot \boldsymbol{\tau}, \tag{101}$$

and for the second system of unknowns $(\mathbf{B}, E)$

$$E - c\mathbf{B} \cdot \boldsymbol{\tau} = h, \tag{102}$$

where $\mathbf{g}$ and h are defined on γ_S. They are linked to the incoming wave via $\mathscr{G}$. When $\mathscr{G} = 0$, the condition (100) is actually a first order absorbing boundary condition. It is often called the Silver–Müller condition. *Without loss of generality*, it is always possible

- to choose the artificial boundary Γ_S such that it does not intersect any of the geometrical singularities, i.e., there exists a neighborhood $\mathscr{V}^j$ of each singularity such that $\mathscr{V}^j \cap \Gamma_S = \emptyset$, for $1 \leqslant j \leqslant N_E$;
- assume that the incoming wave is a smooth field.

Then, the trace $\mathbf{E} \cdot \boldsymbol{\tau}_{|\gamma_S}$ is regular (in a sense which is detailed in [9]): we write it as $\mathbf{E} \cdot \boldsymbol{\tau}_{|\gamma_S} \in H_{\|}^{1/2}(\gamma_S)$.

Let $\widetilde{\mathbf{X}}$ stand for the space of solutions for the electric field, the case of the magnetic one being similar. We have

$$\widetilde{\mathbf{X}} = \{\mathbf{E} \in \mathbf{H}(\mathrm{curl}, \mathrm{div}, \omega), \quad \mathbf{E} \cdot \boldsymbol{\tau} = 0 \qquad \text{on } \gamma_C, \quad \mathbf{E} \cdot \boldsymbol{\tau}_{|\gamma_S} \in H_{\|}^{1/2}(\gamma_S)\}. \tag{103}$$

Like $\mathbf{X}$, $\widetilde{\mathbf{X}}$ is not of H^1-style regularity. Let us thus define $\widetilde{\mathbf{X}}_R$, the regularized subspace of $\widetilde{\mathbf{X}}$:

$$\widetilde{\mathbf{X}}_R = \{\mathbf{E} \in \mathbf{H}^1(\omega), \quad \mathbf{E} \cdot \boldsymbol{\tau} = 0 \text{ on } \Gamma_C\} = \widetilde{\mathbf{X}} \cap \mathbf{H}^1(\omega). \tag{104}$$

The variational formulation (25)–(27) must be modified accordingly. The integration by parts formula, which is used to obtain the formulation, produces new integral terms on γ_S, and the new formulation reads:

Find $(\mathbf{E}, B, \phi) \in \widetilde{\mathbf{X}} \times H_m^1(\omega) \times L_r^2(\omega)$ *such that*

$$\begin{aligned} &\int_\omega \frac{\partial^2 \mathbf{E}}{\partial t^2} \cdot \mathbf{F} r \,\mathrm{d}r\,\mathrm{d}z + c \int_{\gamma_S} \frac{\partial \mathbf{E}}{\partial t} \cdot \boldsymbol{\tau} \mathbf{F} \cdot \boldsymbol{\tau} r \,\mathrm{d}\gamma + c^2 \int_\omega \mathrm{curl}\,\mathbf{E}\mathrm{curl}\,\mathbf{F} r \,\mathrm{d}r\,\mathrm{d}z + \int_\omega \phi \mathrm{div}\,\mathbf{F} r \,\mathrm{d}r\,\mathrm{d}z \\ &\quad = -\frac{1}{\varepsilon_0} \int_\omega \frac{\partial \mathbf{J}}{\partial t} \cdot \mathbf{F} r \,\mathrm{d}r\,\mathrm{d}z + c \int_{\gamma_S} \frac{\partial g}{\partial t} \mathbf{F} \cdot \boldsymbol{\tau} r \,\mathrm{d}\gamma \quad \forall \mathbf{F} \in \widetilde{\mathbf{X}}, \end{aligned} \tag{105}$$

$$\begin{aligned} &\int_\omega \frac{\partial^2 B}{\partial t^2} C r \,\mathrm{d}r\,\mathrm{d}z + \int_{\gamma_S} \frac{\partial B}{\partial t} C r \,\mathrm{d}\gamma + c^2 \int_\omega \mathrm{curl}\, B \cdot \mathrm{curl}\, C r \,\mathrm{d}r\,\mathrm{d}z \\ &\quad = \frac{1}{\varepsilon_0} \int_\omega \mathbf{J} \cdot \mathrm{curl}\, C r \,\mathrm{d}r\,\mathrm{d}z - \int_{\gamma_S} \frac{\partial g}{\partial t} C r \,\mathrm{d}\gamma \quad \forall C \in \times H_m^1(\omega), \end{aligned} \tag{106}$$

$$\int_\omega \operatorname{div} \mathbf{E} q r \,\mathrm{d}r\,\mathrm{d}z = \frac{1}{\varepsilon_0} \int_\omega \mathscr{R} q r \,\mathrm{d}r\,\mathrm{d}z \quad \forall q \in L^2_r(\omega). \tag{107}$$

5.1. A decomposition of the solution in regular and singular parts

It is of importance to note that the singular behavior of the solution is *generated* by the shape of the domain. Thus, it is interesting to keep the same space $\mathbf{X}_\mathrm{S}$ of singular solutions ($\mathbf{X}_\mathrm{S} \subset \widetilde{\mathbf{X}}$). Indeed, one can prove easily that $\widetilde{\mathbf{X}}$ can be decomposed into

$$\widetilde{\mathbf{X}} = \widetilde{\mathbf{X}}_\mathrm{R} \oplus \mathbf{X}_\mathrm{S}, \tag{108}$$

where $\widetilde{\mathbf{X}}_\mathrm{R}$ is the subspace defined by (104). The advantage of using also $\mathbf{X}_\mathrm{S}$ is that it does not depend on the time variable t, and therefore it is computed once and for all (see the remark below).

In practice however, similarly to the case when the whole boundary is a perfect conductor, it is more convenient from a numerical point of view, to use the curl-free subspace $\operatorname{grad} \Phi_\mathrm{S}$ of $\mathbf{X}$ as a basis of the singular fields. As a matter of fact, $\widetilde{\mathbf{X}}$ can also be decomposed into

$$\widetilde{\mathbf{X}} = \widetilde{\mathbf{X}}_\mathrm{R} \oplus \operatorname{grad} \Phi_\mathrm{S}.$$

With this choice, the *SCM* with $\gamma_\mathrm{S} \neq \emptyset$ appears as a slight modification of the formulation obtained with $\gamma_\mathrm{S} = \emptyset$. Indeed, there is no added integral over γ_S in (90) since $\mathbf{v}^i_\mathrm{S} \cdot \boldsymbol{\tau} = 0, 1 \leqslant i \leqslant N_\mathrm{E}$, and Eq. (89) is unchanged.

Concerning Eq. (88), there is an additional term in the right-hand side if $g \neq 0$, and in all the cases an additional term

$$c \int_{\gamma_\mathrm{S}} \frac{\partial \mathbf{E}_\mathrm{R}}{\partial t} \cdot \boldsymbol{\tau} \mathbf{F}_\mathrm{R} \cdot \boldsymbol{\tau} r \,\mathrm{d}\gamma$$

in the left-hand side. These one or two supplementary terms are not specific to the *SCM* and appear also in regular domains.

There remains to semi-discretize in space, which is done in a way similar to the one of the perfectly conducting boundary case, the main modification being the addition to the left-hand side of (91) of

$$c \frac{\mathrm{d}}{\mathrm{d}t} \mathbb{M}_{\gamma_\mathrm{S}} \vec{\mathsf{E}}_\mathrm{R},$$

where $\mathbb{M}_{\gamma_\mathrm{S}}$ denotes the boundary mass matrix associated to the term $\int_{\gamma_\mathrm{S}} \mathbf{E}_\mathrm{R} \cdot \boldsymbol{\tau} \mathbf{F}_\mathrm{R} \cdot \boldsymbol{\tau} r \,\mathrm{d}\gamma$.

We then perform a time discretization involving the same scheme as in Section 4.3. Except the right-hand sides if $g \neq 0$, the only modification compared to (94)–(96) consists in replacing $\mathbb{M}_\omega$ by $\mathbb{M}_\omega + c(\Delta t/2)\mathbb{M}_{\gamma_\mathrm{S}}$. The resulting linear system is solved as previously with no additional effort, recalling that the boundary mass matrix $\mathbb{M}_{\gamma_\mathrm{S}}$ is block-diagonal thanks to a quadrature formula which preserves the accuracy (see [5] for details).

The system for the magnetic field is solved in the same way.

6. Numerical results

In this section, we present numerical tests of both electric and magnetic field computations, that allows to evaluate the code-related performances of the *Singular Complement Method* (*SCM*) in axisymmetric

domains. The bases of grad Φ_S and $\mathbf{W}_S$ are computed during the initialization step, together with the regular–singular and singular–singular matrices. Further, updating the values of the singular coefficients $(\kappa^i)_{i=1,N_E}$ and $(\delta^j)_{j=1,N_B}$ requires O(1) operations per time-step. Therefore, the additional memory requirements, and computing effort, are small.

Since analytical solutions are not available, we have chosen to compare the numerical results to those computed by other codes.

6.1. Computation of a basis of W_S and grad Φ_S

Let us consider the top hat domain Ω with a reentrant circular edge, that corresponds to an L-shaped domain ω with one reentrant corner. To compute the magnetic basis $\mathbf{w}_S$ of $\mathbf{W}_S$, we introduce an unstructured mesh of ω made up of triangles, with no particular mesh refinement near the corner. Following the method exposed in Section 4.1.1, we first compute the dual singular function P_S, to obtain $\mathbf{w}_S$ from the potential ψ_S.

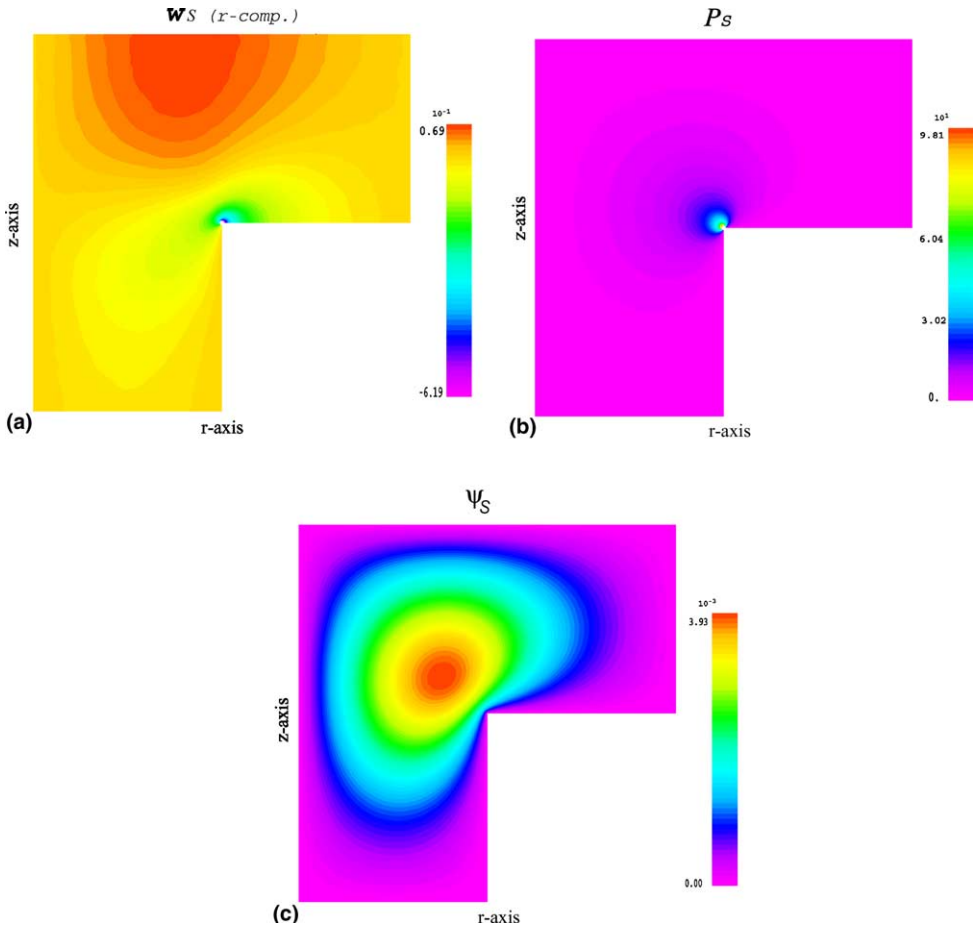

Fig. 4. Computed bases in the magnetic case.

The solutions are pictured in Fig. 4. When representing functions or fields with a singular behavior, instead of truncating the results, we have chosen to exclude the (infinite) singular node value, so as not to "flatten" the image by an arbitrary truncation value.

In Fig. 4(a), one can see that the SCM captures well the field $\mathbf{w}_S \in \mathbf{W}_S$ near the edge (and far away from it). Again, a conforming P^1 Finite Element Method can not yield such a result. In addition, the results are not noisy, even though the mesh is not particularly refined near the edge. In Fig. 4(b), one can check that the method is also efficient to compute the most singular term P_S. Last, the result on the smooth function ψ_S (see Fig. 4(c)), shows that the method is efficient for more regular functions or fields: in that, it generalizes the singular function method.

Now when dealing with a basis of grad Φ_S for the electric field, we consider another axisymmetric domain Ω which consists in a cylinder, at the top of which a cone of revolution was removed. Its intersection with a meridian half-plane is the computational domain ω (see Fig. 5), that allows us to illustrate the computation of electric singular basis due to conical points. Here again, this domain is approximated by a mesh with no particular mesh refinement near the conical point, and $\mathbf{v}_S$ is evaluated as previously, by computing first the dual singular function p_S, and finally $\mathbf{v}_S$ from the potential ϕ_S.

The results are depicted in Fig. 5(a) and the conclusions are similar to the $\mathbf{w}_S$ case.

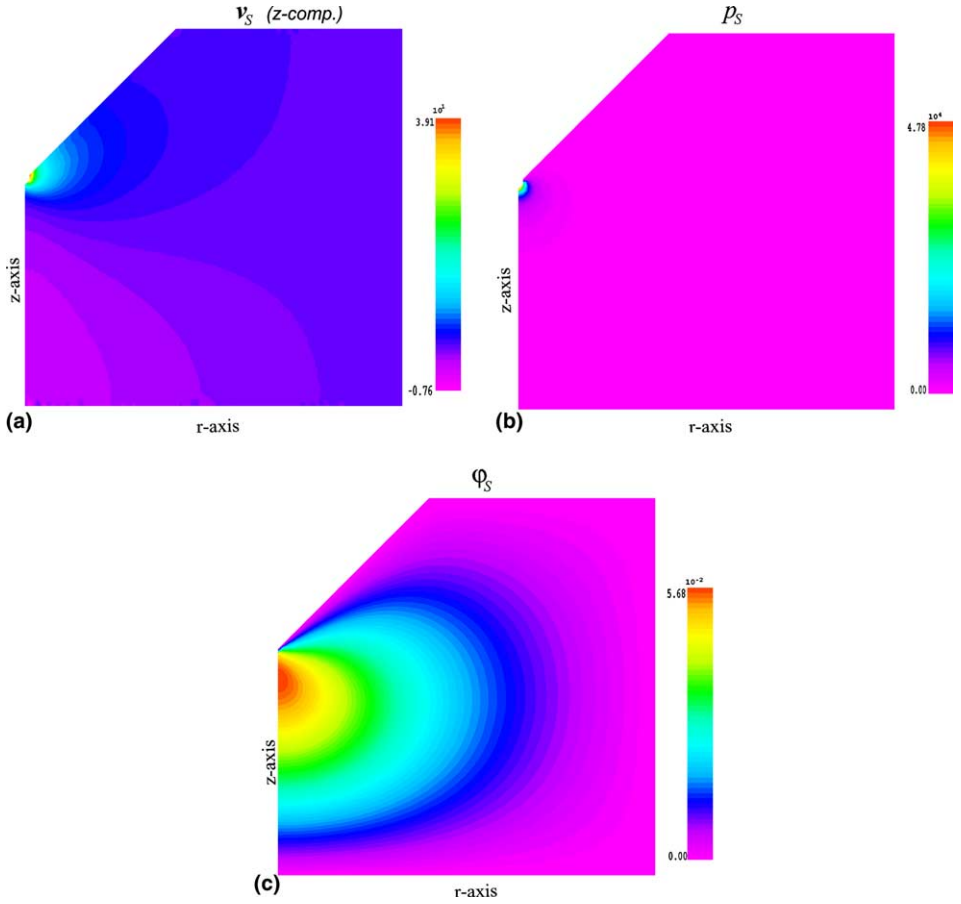

Fig. 5. Computed bases in the electric case.

6.2. Time-dependent cases

In this section, the quality of the *SCM* is evaluated numerically in cases representative of situations that can occur when one is dealing with electromagnetic axisymmetric fields.

In the first instance, one computes the electromagnetic singular field generated by a current loop. Next, it is well known that commonly studied devices such as hyperfrequency systems often include waveguides, either to conduct the field that excites particles, or to conduct the field induced by them. So, in the second example, the propagation of an electromagnetic wave near a singular conical point is investigated.

6.2.1. Example with a current

In this first instance, we consider the same L-shaped domain ω as for the computation of $\mathbf{W}_S$ (corresponding to a top hat domain Ω), on which a perfectly conducting boundary condition is imposed. We are interested in computing the electromagnetic field $(\mathbf{B}, E)$ created by a current loop. The initial conditions are set to zero. The current is defined as $\mathscr{J}(\mathbf{x}, t) = J_\theta \mathbf{e}_\theta$, $J_\theta = 10\sin(\lambda t)$, with a frequency $\lambda/2\pi = 2.5 \times 10^9$ Hz. The support of this current is a little disc centered at the middle of the domain.

This current generates a wave which propagates circularly around the current source. Physically, as long as the wave has not reached the reentrant corner, the field is smooth. Let t_s be the impact time, then, if one writes

$$\mathbf{B}(\mathbf{x}, t) = \mathbf{B}_R(\mathbf{x}, t) + \kappa(t)\mathbf{w}_S(\mathbf{x}),$$

$\kappa(t)$ is equal to zero for all t lower than t_s, and so $\mathbf{B}_R(\mathbf{x}, t)$ and $\mathbf{B}(\mathbf{x}, t)$ coincide. Now, on the one hand, for t greater than t_s, $\kappa(t) \neq 0$ and the support of $\mathbf{w}_S$ being non-local (in fact, the support of $\mathbf{w}_S$ spans the whole of ω), one has $\kappa(t)\mathbf{w}_S(\mathbf{x}) \neq 0$, for all $\mathbf{x} \in \omega$ and $t > t_s$. On the other hand, however, one wishes to reproduce the obvious physical behavior, which is that for any point $\mathbf{x}$ and time t, $\mathbf{B}(\mathbf{x}, t) = 0$ if $t < t_\mathbf{x}$, where $t_\mathbf{x}$ denotes the time at which the wave reaches $\mathbf{x}$.

One can check (see Fig. 6) that $\mathbf{B}_R(\mathbf{x}, t)$ takes non-zero values, and therefore that it "compensates" for $\kappa(t)\mathbf{w}_S(\mathbf{x})$, i.e., $\mathbf{B}_R(\mathbf{x}, t) = -\kappa(t)\mathbf{w}_S(\mathbf{x})$. Thus, $\mathbf{B}(\mathbf{x}, t)$ remains equal to zero while $t_s < t < t_\mathbf{x}$.

The same computation has been carried out via the classical nodal FE code (without the *SCM*) and has been compared. In Fig. 7, the isovalues of the radial components of the magnetic field are pictured (with identical scales). It shows a most unlikely approximation of the true solution (no singular behavior).

Because it is not possible to provide an analytical solution, we compare our results to the computations made by another code, based on *Finite Volume* (*FV*) techniques *à la* Delaunay–Voronoi [17].

As mentioned in the introduction, this method allows to approximate the solution in a neighborhood of the reentrant corner (with an appropriate mesh refinement), the degrees of freedom being located on the edges. The Fig. 8 shows the isovalues of the magnetic field (B_z component after 1000 time steps), which has been computed by the two methods on the same mesh. The results obtained by both methods are comparable, which shows the feasibility of the *SCM* in axisymmetric cases. Moreover, the *SCM* provides a numerical solution which is less noisy. Last, the results obtained by both methods on the smooth (cf. [2]) component E of the electric field are almost identical. This emphasizes once more that the differences come from the singular part.

6.2.2. The waveguide case

In this last example, the propagation of an electromagnetic wave, namely $(\mathbf{E}, B)$, in a geometry with a singular conical point, is studied numerically. This case provides an interesting illustration of the possibilities of the method, when it is used on a more "complete" formulation, that is with different types of boundary conditions. We consider a coaxial cylindrical waveguide in which the inner cylindrical part ends with a conical point. The geometry and the data do not depend on the variable θ. The computational domain ω, that is the meridian section of the waveguide, is pictured in Fig. 9.

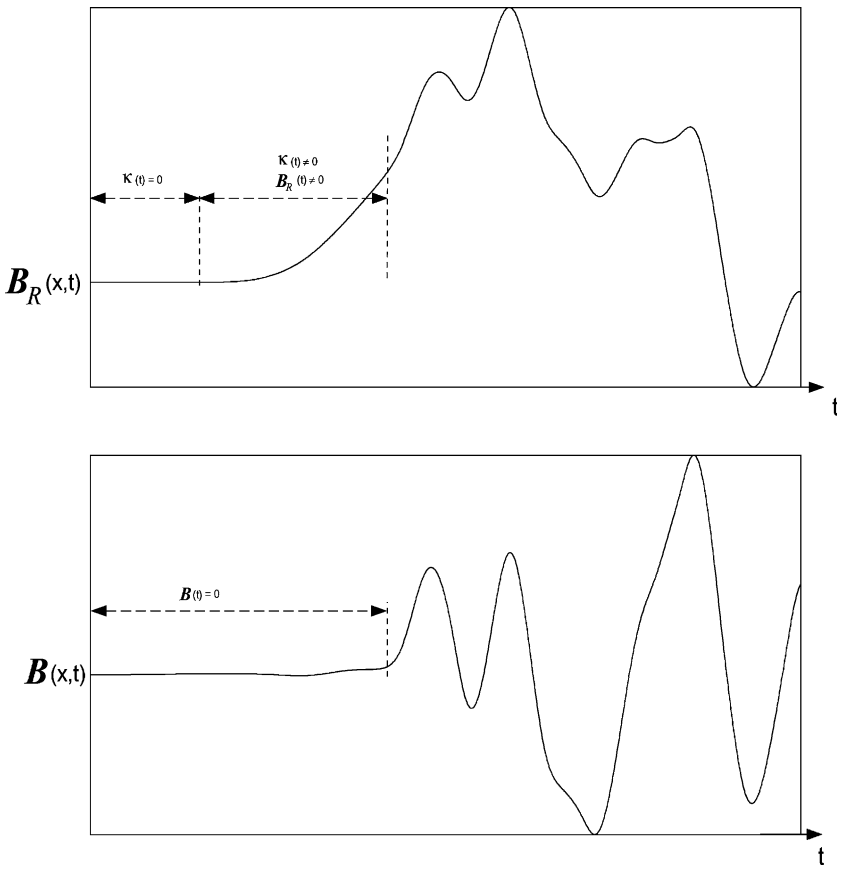

Fig. 6. At a given point $\mathbf{x}$, comparison of the radial components of $\mathbf{B}_{\mathrm{R}}(\mathbf{x},t)$ (top) and $\mathbf{B}(\mathbf{x},t)$ (bottom) with t varying.

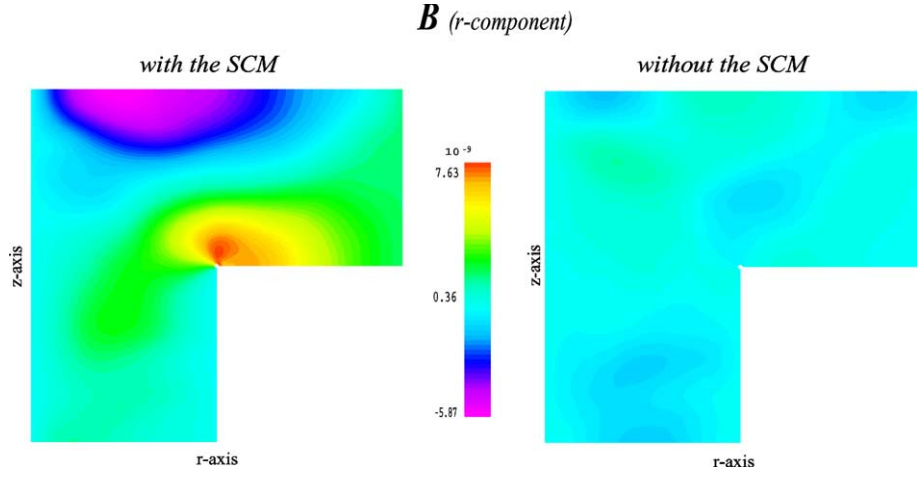

Fig. 7. Component B_r, computed with the *SCM* (left) and without the *SCM* (right).

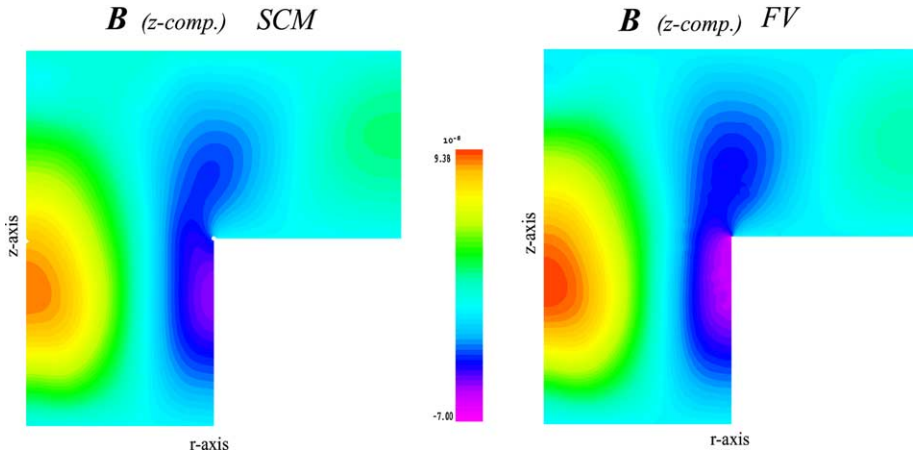

Fig. 8. Component B_z, computed by the *SCM* (left) and by the *FV* (right).

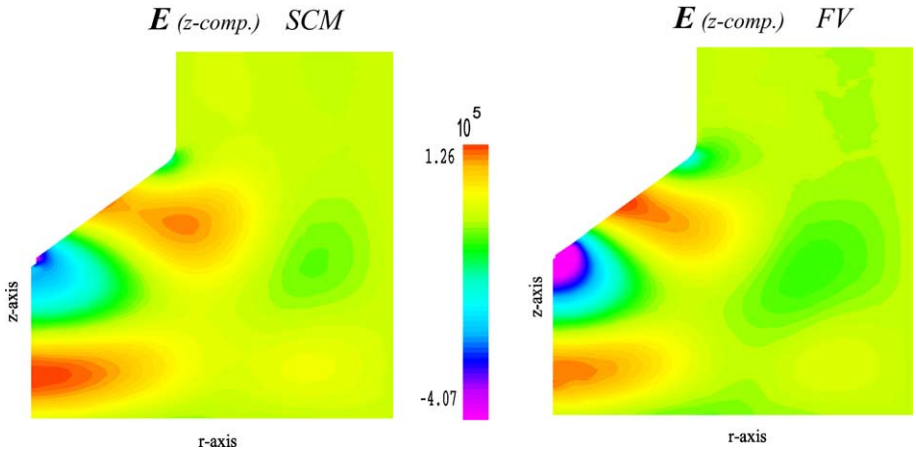

Fig. 9. Component E_z, computed by the *SCM* (left) and by the *FV* (right).

An incident wave enters the waveguide through the boundary γ_s^1 (at the bottom), and leaves the domain through γ_s^2 (at the top). This behavior is modeled thanks to the boundary condition (101), which is expressed as

$$\mathbf{E}\cdot\boldsymbol{\tau} - cB = g, \quad g(t)_{|\gamma_s^1} = C\sin(\lambda t), \quad g(t)_{|\gamma_s^2} = 0, \tag{109}$$

where C is a constant and λ is associated to the frequency 2.5×10^9 Hz. At the initial time $t=0$, the electromagnetic field is equal to zero all over the guide. As in the preceding case, the field is smooth until the wave reaches the reentrant corner, and then it becomes singular.

As previously, the result has been compared to that produced by the FV code. Fig. 9 depicts the isovalues of the longitudinal component of the electric field after 600 time-steps.

Once again, the SCM provides a numerical solution which is globally less noisy, and more precise in the neighborhood of the corner. Last, the results are almost identical for B.

7. Conclusion

In this paper, we presented the generalization to axisymmetric problems of a method we developed – the *Singular Complement Method* – to solve Maxwell equations in a non-smooth and a non-convex domain.

It is based on a splitting of the space of solutions with respect to regularity, in a regular subspace, which is equal to the entire space when the domain is smooth or convex, and a singular subspace. In this axisymmetric situation, the mathematical analysis (finite dimension of the singular subspaces, characterization of the singularities, etc.) has been carried out and is already published ([2,3]).

The generalization of the *SCM* to the axisymmetric case is not a straightforward extension of the two-dimensional Cartesian one. Indeed, even in convex or smooth domains, a classical Finite Element approach requires special attention due to the weighted measure $r\,\mathrm{d}r\,\mathrm{d}z$. Particularities due to conical points, causing specific difference between the electric and magnetic cases also appear, for example in the choice of the singular subspace well adapted to computations, etc.

Numerical methods have been proposed, based on the P_1 Lagrange finite element approximation for the regular part of the solutions, and on special additional test-functions, which are used to capture numerically the singular part of the solution.

Results of simulations have been shown to illustrate the efficiency of the *SCM* in a series of examples based on practical three-dimensional axisymmetric devices. In particular, the use of a non-divergence-free decomposition for the electric field proves that the *SCM* can be coupled to particle methods in axisymmetric situations, as in the bidimensional case (cf. [1]).

Currently we devote our attention to the (non-axisymmetric) three-dimensional domains. The theoretical aspects are under control and there remains now to provide an effective approximation of the singular part of the solution. As a matter of fact, in the 3D case, this singular part belongs to an infinite dimensional space.

Finally, the *SCM* proved to be easy to implement, as it can be included in already existing codes, without having to rewrite them in their entirety, for low additional memory requirements and small additional cpu costs.

Appendix A. Operators in cylindrical coordinates

$$\operatorname{grad} f = \frac{\partial f}{\partial r}\mathbf{e}_r + \frac{1}{r}\frac{\partial f}{\partial \theta}\mathbf{e}_\theta + \frac{\partial f}{\partial z}\mathbf{e}_z, \tag{110}$$

$$\operatorname{div} \mathbf{u} = \frac{1}{r}\frac{\partial}{\partial r}(ru_r) + \frac{1}{r}\frac{\partial u_\theta}{\partial \theta} + \frac{\partial u_z}{\partial z}, \tag{111}$$

$$\operatorname{curl} \mathbf{u} = \left(\frac{1}{r}\frac{\partial u_z}{\partial \theta} - \frac{\partial u_\theta}{\partial z}\right)\mathbf{e}_r + \left(\frac{\partial u_r}{\partial z} - \frac{\partial u_z}{\partial r}\right)\mathbf{e}_\theta + \frac{1}{r}\left(\frac{\partial}{\partial r}(ru_\theta) - \frac{\partial u_r}{\partial \theta}\right)\mathbf{e}_z, \tag{112}$$

$$\Delta f = \frac{\partial^2 f}{\partial r^2} + \frac{1}{r}\frac{\partial f}{\partial r} + \frac{1}{r^2}\frac{\partial^2 f}{\partial \theta^2} + \frac{\partial^2 f}{\partial z^2} \tag{113}$$

$$\nabla \mathbf{u} = \begin{pmatrix} \frac{\partial u_r}{\partial r} & \frac{1}{r}\left(\frac{\partial u_r}{\partial \theta} - u_\theta\right) & \frac{\partial u_r}{\partial z} \\ \frac{\partial u_\theta}{\partial r} & \frac{1}{r}\left(\frac{\partial u_\theta}{\partial \theta} + u_r\right) & \frac{\partial u_\theta}{\partial z} \\ \frac{\partial u_z}{\partial r} & \frac{1}{r}\frac{\partial u_z}{\partial \theta} & \frac{\partial u_z}{\partial z} \end{pmatrix}. \tag{114}$$

References

[1] F. Assous, P. Ciarlet Jr., E. Garcia, Résolution des équations de Maxwell instationnaires avec charges dans un domaine bidimensionnel, C. R. Acad. Sci. Paris, t. 330 (Série I) (2000) 391.
[2] F. Assous, P. Ciarlet Jr., S. Labrunie, Theoretical tools to solve the axisymmetric Maxwell equations, Math. Methods Appl. Sci. 25 (2002) 49–78.
[3] F. Assous, P. Ciarlet Jr., S. Labrunie, Solution of axisymmetric Maxwell equations, Math. Methods Appl. Sci. 26 (2003) 861–896.
[4] F. Assous, P. Ciarlet Jr., J. Segré, Numerical solution to the time-dependent Maxwell equations in two-dimensional singular domain: the singular complement method, J. Comput. Phys. 161 (2000) 218–249.
[5] F. Assous, P. Degond, E. Heintzé, P.A. Raviart, J. Segré, On a finite element method for solving the three-dimensional Maxwell equations, J. Comput. Phys. 109 (1993) 222–237.
[6] F. Assous, P. Degond, J. Segré, Numerical approximation of the Maxwell equations in inhomogeneous media by a P^1 conforming finite element method, J. Comput. Phys. 128 (1996) 363–380.
[7] H. Blum, M. Dobrowolski, On finite element methods for elliptic equations on domains with corners, Computing 28 (1982) 53–63.
[8] A.-S. Bonnet-Bendhia, M. Dauge, K. Ramdani, Spectral analysis and singularities of a non-coercive transmission problem, C. R. Acad. Sci. Paris, t. 328 (Série I) (1999) 717–720.
[9] A. Buffa, P. Ciarlet Jr., On traces for functional spaces related to Maxwell's equations. Part I: an integration by parts formula in Lipschitz polyhedra, Math. Methods Appl. Sci. 24 (2001) 9–30.
[10] P. Ciarlet Jr., V. Girault, Condition inf-sup pour l'élément fini de Taylor-Hood P_2-iso-P_1, 3-D; application aux équations de Maxwell, C. R. Acad. Sci. Paris, t. 335 (Série I) (2002) 827–832.
[11] P. Ciarlet Jr., J. He, The singular complement method for 2D scalar problems, C. R. Acad. Sci. Paris, t. 336 (Série I) (2003) 353–358.
[12] M. Costabel, M. Dauge, Maxwell and Lamé eigenvalues on polyhedra, Math. Methods Appl. Sci. 22 (1999) 243–258.
[13] A. Elmkies, P. Joly, Eléments finis d'arete et condensation de masse pour les équations de Maxwell: le cas de dimension 3, C. R. Acad. Sci. Paris, t. 325 (Série I) (1997) 1217–1222.
[14] M. Fortin, R. Glowinski, Augmented Lagrangian Methods, Springer Series in Computational Mathematics, 5, 1986.
[15] W.W. Hager, Updating the inverse of a matrix, SIAM Rev. 31 (1989) 221–239.
[16] C. Hazard, S. Lohrengel, A singular field method for Maxwell's equations: numerical aspects for 2D magnetostatics, SIAM J. Appl. Math. 40 (2002) 1021–1040.
[17] F. Hermeline, Two coupled particle-finite volume methods using Delaunay–Voronoi meshes for the approximation of Vlasov–Poisson and Vlasov–Maxwell equations, J. Comput. Phys. 106 (1990) 1–18.
[18] M.A. Moussaoui, Sur l'approximation des solutions du problme de Dirichlet dans un ouvert avec coins, in: P. Grisvard, W. Wendland, J.R. Whiteman (Eds.), Singularities and Constructive Methods for their Treatment, Lecture Notes in Mathematics, 1121, Springer Verlag, Berlin, 1984.
[19] S.A. Nazarov, B.A. Plamenevsky, Elliptic problems in domains with piecewise smooth boundaries, De Gruyter Exp. Math. 13 (1994).
[20] J.C. Nédélec, Mixed finite elements in $\mathbb{R}^3$, Numer. Math. 35 (1980) 315–341.
[21] J.C. Nédélec, A new family of mixed finite elements in $\mathbb{R}^3$, Numer. Math. 50 (1986) 57–81.
[22] O.C. Zienkiewicz, La Méthode Des Éléments Finis Appliquée à L'art De L'ingénieur, Ediscience, Paris, 1973.